รายงานวิจัยฉบับสมบูรณ์

โครงการ “ผลึกนาโนกระดูกเทียมเพื่อเป็นวัสดุการแพทย์”

โดย ผศ.ดร ศิวพร มีจู

ธันวาคม 2551

สัญญาเลขที่ **MRG5080059**

รายงานวิจัยฉบับสมบูรณ์

โครงการ “**ผลึกนาโนกระดูกเทียมเพื่อเป็นวัสดุการแพทย์**”

ผศ. ดร. ศิวพร มีจู
ภาควิชาเคมี คณะวิทยาศาสตร์ มหาวิทยาลัยมหิดล

สนับสนุนโดยสำนักงานกองทุนสนับสนุนการวิจัย

(ความเห็นในรายงานนี้เป็นของผู้วิจัย สกว.ไม่จำเป็นต้องเห็นด้วยเสมอไป)

รูปแบบ Abstract (บทคัดย่อ)

Project Code : MRG5080059

Project Title : Nanocrystalline Hydroxyapatite for Medical Applications

Investigator : Asst. Prof. Siwaporn Meejoo
Department of Chemistry, Faculty of Science, Mahidol University

E-mail Address : scsmj@mahidol.ac.th

Project Period : 48 months

A one-step chemical reaction to obtain a hydroxyapatite/collagen (HAp/Col) composite was accomplished. The highly porous HAp/Col hybrid material is of globular structure on a rod-like, polycrystal platform, with the length of crystals about 6-8 μm. Formation of the composite was driven not only by the mineralization of HAp crystals but also by interfacial interactions between ions on the HAp surface and residual ions on the Col. IR absorption bands corresponding to hydroxyl and phosphate groups provided convincing evidence of the mineralization of HAp in the Col matrix. In vitro bioactivity of the HAp/Col was examined by soaking the composite in a simulated body fluid (SBF) solution. The precipitation of agglomerated HAp crystals on the surface of the HAp/Col surface illustrated the biological compatibility of the composite. Surface morphology of HAp/Col showed substantially large cavities which are suitable for drug delivery applications. This work has shown that an antibiotic was well-stabilized within pores and on the surface of the composite and suggested that this composite has a high potential for drug-delivery applications.

Keywords : Biomaterials, Chemical synthesis, Powder diffraction, Microstructure

บทคัดย่อ

รหัสโครงการ : MRG5080059

ชื่อโครงการ : ผลึกนาโนกระดูกเทียมเพื่อเป็นวัสดุการแพทย์

ชื่อนักวิจัย และสถาบัน : ผศ. ดร. ศิวพร มีจู
ภาควิชาเคมี คณะวิทยาศาสตร์ มหาวิทยาลัยมหิดล

E-mail Address : scsmj@mahidol.ac.th

ระยะเวลาโครงการ : 48 เดือน

จากปฏิกิริยาเคมีเพียงขั้นตอนเดียวสามารถเตรียมวัสดุคอมโพสิตไฮดรอกซีอะพาไทท์/คอลลาเจนที่มีลักษณะโครงสร้างจุลภาคที่น่าสนใจ กล่าวคือมีส่วนที่มีรูปทรงกลมบนฐานของผลึกรูปแท่งที่มีขนาดยาวประมาณ 6-8 ไมโครเมตร วัสดุคอมโพสิตที่เตรียมได้เกิดเนื่องมาจากแรงพื้นผิวระหว่างไอออนบนพื้นผิวของไฮดรอกซีอะพาไทท์กับไอออนบนผิวคอลลาเจน ผลจากไออาร์สเปกตรัมยืนยันพันธะเคมีของกลุ่มไฮดรอกซี และกลุ่มฟอสเฟตที่แสดงให้เชื่อว่ามีไฮดรอกซีอะพาไทท์อยู่ในคอลลาเจน การวิเคราะห์สมบัติชีวภาพของวัสดุดังกล่าวดำเนินการโดยการแช่วัสดุคอมโพสิตในสารละลายที่เลียนแบบสารละลายพลาสมาในร่างการมนุษย์ พบว่ามีกลุ่มผลึกของไฮดรอกซีอะพาไทท์มาเกาะบนผิววัสดุคอมโพสิตซึ่งยืนยันถึงสมบัติชีวภาพของคอมโพสิต เนื่องจากโครงสร้างของวัสดุคอมโพสิตมีความเป็นรูพรุนและช่องว่างสูง จึงมีความเป็นไปได้ในการใช้ในงานประยุกต์ระบบส่งยา งานวิจัยครั้งมีแสดงให้เห็นว่าสามารถที่จะเติมตัวยาแก้อักเสบที่บริเวณผิวและในโครสร้างของวัสดุคอมสิตไฮดรอกซีอะพาไทท์/คอลลาเจนได้เป็นอย่างดี

คำหลัก : วัสดุชีวภาพ การสังเคราะห์เชิงเคมี การลี้ยวเบนรังสีเอ็กซ์ของผงตัวอย่าง
โครงสร้างระดับจุลภาค

Executive Summary

1. ความสำคัญและที่มีของปัญหา

การพัฒนาทางการแพทย์ด้านกระดูก ได้แก่ การเชื่อมต่อกระดูก (Bone grafting) การเหนี่ยวนำการสร้างกระดูกใหม่ (Bone reconstruction) รวมทั้งการพัฒนาด้านทันตกรรม ได้รับความ สนใจเป็นอย่างมาก ยังผลให้เกิดการเร่งพัฒนาและวิจัยวัสดุทางการแพทย์ประเภทใหม่ๆ ขึ้น โดยเฉพาะอย่างยิ่ง วัสดุนาโนคอมโพสิต เนื่องจากการรักษาผู้ป่วยด้วยวิธีปลูกถ่ายกระดูก นั้น ถึงแม้จะเป็นวิธีที่ได้รับการยอมรับมานาน แต่มักมีข้อจำกัดได้แก่ ขาดผู้บริจาคที่เหมาะสม และ ปัญหาการติดเชื้อ ทำให้เกิดการพัฒนาสังเคราะห์วัสดุทางชีวภาพ (Biomaterials) เพื่อใช้แทนการ ปลูกถ่ายกระดูกจากผู้บริจาค แต่วัสดุสังเคราะห์ส่วนใหญ่มีโครงสร้างและองค์ประกอบแตกต่างจาก กระดูกจริงอย่างสิ้นเชิง ดังนั้นการพัฒนาวัสดุแทนกระดูกจริงในปัจจุบัน มุ่งเน้นให้ได้วัสดุใหม่ที่มี โครงสร้างและองค์ประกอบคล้ายคลึงกับกระดูกจริงให้มากที่สุด และสามารถคงอยู่ในร่างกาย กลมกลืนกับกระดูกและเนื้อเยื่อส่วนอื่นอีกด้วย

สารประกอบ ไฮดรอกซีอาพาไทท์ (hydroxyapatite) มีองค์ประกอบเดียวกับสารประกอบที่พบในกระดูกและฟันของสัตว์เลี้ยงลูกด้วยนม จึงถูกเรียกว่าเป็นกระดูกเทียมที่มีสมบัติที่เข้ากันได้ทางชีวภาพ (Bio-compatibility) มีความคงทน (stability) และความเฉื่อย (inertness) จึงจัดว่าเป็นวัสดุที่ได้รับความสนใจสูงที่สุดทางการแพทย์ด้านกระดูกและฟัน และหากจะพัฒนาวัสดุใหม่ให้มีลักษณะใกล้เคียงกับกระดูกจริง ควรได้แก่ วัสดุคอมโพสิตระหว่าง Hydroxyapatite และ Collagen ด้วยในปัจจุบันการปรับเปลี่ยนโครงสร้างและองค์ประกอบ และการตรวจสอบ สามารถทำได้ถึงระดับอะตอมหรือโมเลกุล (Nanotechnology) จึงทำให้มีความเป็นไปได้ในการเตรียมวัสดุนาโน คอมโพสิต Hydroxyapatite/Collagen ที่มีสมบัติพิเศษกว่าวัสดุคอมโพสิตทั่วไปโครงการวิจัยนี้มุ่งหวังที่จะรายงานและอธิบายผลการทดลองเพื่อเป็นองค์ความรู้ใหม่ ได้แก่ หลักการออกแบบวัสดุนาโนคอมโพสิต Hydroxyapatite/Collagen เชื่อมโยงสมบัติกายภาพ และ ชีวภาพกับโครงสร้างและองค์ประกอบของวัสดุทางการแพทย์ให้มีสมบัติเฉพาะเหมาะสมกับการ รักษาในแต่ละกรณี ซึ่งจะทำให้มีความก้าวหน้าในเชิงวิชาการทั้งทางด้านวิทยาศาสตร์นาโน เคมี เชิง ฟิสิกส์ วัสดุศาสตร์ รวมทั้งงานวิจัยด้านเคมีคลินิก ซึ่งยังไม่มีการรายงานมาก่อน

2. วัตถุประสงค์

(1) เพื่อศึกษาผลของการนำผลึกนาโนกระดูกเทียมเตรียมวัสดุคอมโพสิตชีวภาพ ต่อสมบัติกายภาพ และ สมบัติชีวภาพของวัสดุคอมโพสิต

(2) เพื่ออธิบายหลักการการปรับเปลี่ยนสมบัติของวัสดุคอมโพสิตที่เตรียมจากผลึกนาโนกระดูกเทียม เชื่อมโยงกับโครงสร้าง นำไปสู่การออกแบบวัสดุให้มีประโยชน์ตามความต้องการได้

(3) เพื่อเผยแพร่องค์ความรู้ และสร้างเครือข่ายการวิจัยร่วมกับนักวิจัยทางการแพทย์ในประเทศเพื่อการพัฒนาวัสดุทางการแพทย์

เนื้อหางานวิจัย

งานวิจัยแบ่งตามงาน 3 หัวข้อสอดคล้อง Output ของงานวิจัยที่ได้รับการสนับสนุนทุนวิจัยจาก สกว. ได้แก่

1. การเตรียมและศึกษาสมบัติของวัสดุคอมโพสิตไฮดรอกซีอะพาไทท์/คอลลาเจน
2. การเตรียมและศึกษาสมบัติวัสดุไฮดรอกซีอะพาไทท์ที่มี Fe แทนที่ Ca
3. สมบัติการดูดซับโลหะของมัลติวอล คาร์บอนนาโนทิวบ์

โดยในหัวข้อ 1-2 มี ขั้นตอนการดำเนินงานวิจัยมีดังนี้

(1) จัดหาวัสดุได้แก่ Collagen ที่รู้สมบัติและองค์ประกอบคงตัวแน่นอน
(2) สังเคราะห์ผลึกนาโนกระดูกเทียม (Nanocrystalline Hydroxyapatite) ด้วยกระบวนการ Assisted Microwave irradiation co-precipitation
(3) วัดสมบัติกายภาพ และสมบัติเทอร์โมไดนามิกส์ของ Collagen
(4) เตรียมวัสดุคอมโพสิตชีวภาพ ระหว่าง Collagen และ ผลึกนาโนกระดูกเทียม
(5) วัดสมบัติกายภาพ และสมบัติเทอร์โมไดนามิกส์ของวัสดุคอมโพสิตชีวภาพ ดังข้อ (3)
(6) วิเคราะห์ข้อมูลที่ได้จากผลการทดลองในข้อ (5)
(7) สรุปผลการวิจัย

ทั้งนี้การเตรียม ได้มีการเติม Fe ไอออนในระหว่างการเตรียมไฮดรอกซีอะพาไทท์โดยกระบวนการขั้นตอน (2) และหัวข้อที่ 3 มี ขั้นตอนการดำเนินงานวิจัยมีดังนี้

(1) จัดหา คาร์บอนนาโนทิวบ์ โดยได้รับการอนุเคราะห์จากมหาวิทยาลัยเชียงใหม่
(2) ศึกษาสมบัติโครงสร้างและสมบัติกายภาพของตัวอย่างคาร์บอนนาโนทิวบ์
(3) กำจัด Nickel ซึ่งตกค้างจากการสังเคราะห์ออกจากคาร์บอนนาโนทิวบ์
(4) นำคาร์บอนนาโนทิวบ์จากข้อ (1) มาบดด้วยวิธี ball-mill
(5) ทดสอบความสามารถการดูดซับโลหะเปรียบเทียบระหว่างคาร์บอนนาโนทิวบ์จากข้อ (1) (4) และ (5)
(6) วิเคราะห์ข้อมูลจากผลการทดลอง
(7) สรุปผลการวิจัย

<u>สรุปผลงานวิจัย</u>

1. การเตรียมและศึกษาสมบัติของวัสดุคอมโพสิตไฮดรอกซีอะพาไทท์/คอลลาเจน

ได้สังเคราะห์และศึกษาสมบัติโครงสร้าง สมบัติชีวภาพ และการเป็นระบบส่งยาของวัสดุคอมโพสิตไฮดรอกซีอะพาไทท์/คอลลาเจน มีรายละเอียดแนบในภาคผนวก

2. การเตรียมและศึกษาสมบัติวัสดุไฮดรอกซีอะพาไทท์ที่มี Fe แทนที่ Ca

ได้สังเคราะห์และศึกษาสมบัติโครงสร้าง สมบัติชีวภาพ และสมบัติเชิงกลของ วัสดุไฮดรอกซีอะพาไทท์ที่มี Fe แทนที่ Ca มีรายละเอียดแนบในภาคผนวก

3. สมบัติการดูดซับโลหะของมัลติวอล คาร์บอนนาโนทิวบ์

ได้ปรับเปลี่ยนโครงสร้างของมัลติวอล คาร์บอนนาโนทิวบ์ ด้วยกรรมวิธิเคมี และกรรมวิธีเชิงกล และตรวจสอบสมบัติการดูดซับโลหะของตัวอย่างคาร์บอนนาโนทิวบ์ มีรายละเอียดแนบในภาคผนวก

Output จากโครงการวิจัยที่ได้รับทุนจาก สกว.

1. ผลงานตีพิมพ์ในวารสารวิชาการนานาชาติ (ระบุชื่อผู้แต่ง ชื่อเรื่อง ชื่อวารสาร ปี เล่มที่ เลขที่ และหน้า) หรือผลงานตามที่คาดไว้ในสัญญาโครงการ

   1.1 S. Meejoo, W. Pon-On, S. Charnchai and T. Amornsakchai, Substitution of Iron in Preparation of Enhanced Thermal Property and Bioactivity of Hydroxyapatite, *Advanced Materials Research* 55-57, 689-692 (2008)

   1.2 Weeraphat Pon-On, Siwaporn Meejoo and I-Ming Tang, Formation of hydroxyapatite crystallites using organic template of polyvinyl alcohol (PVA) and sodium dodecyl sulphate (SDS), *Materials Chemistry and Physics*, 12(2), 453-460 (2008)

   1.3 U. Rinzin, P. Singjai, P. Wilairat and S. Meejoo, Mechanochemical Treated Multi-walled Carbon Nanotubes for Incorporation of Metal Ions, *Advanced Materials Research* 55-57, 537-540 (2008)

   1.4 Siwaporn Meejoo, Weeraphat Pon-On, Taweechai Amornsakchai, Highly porous Hydroxyapatite/collagen composite derived by self-organized mineralization, Materials Chemistry and Physics, 2008 Submitted

2. การนำผลงานวิจัยไปใช้ประโยชน์
   - เชิงวิชาการ (มีการพัฒนาการเรียนการสอน/สร้างนักวิจัยใหม่)

3. อื่นๆ (เช่น ผลงานตีพิมพ์ในวารสารวิชาการในประเทศ การเสนอผลงานในที่ประชุมวิชาการ หนังสือ การจดสิทธิบัตร)

   เสนอผลงานแบบปากเปล่า International Conference on Smart Materials – Smart/Intelligent Materials and Nano Technology & 2nd International Workshop on Functional Materials and Nanomaterials จ.เชียงใหม่ ระหว่างวันที่ 22-25 เมษายน 2551

ภาคผนวก

Materials Chemistry and Physics xxx (2008) xxx–xxx

Contents lists available at ScienceDirect

Materials Chemistry and Physics

journal homepage: www.elsevier.com/locate/matchemphys

Formation of hydroxyapatite crystallites using organic template of polyvinyl alcohol (PVA) and sodium dodecyl sulfate (SDS)

Weeraphat Pon-On[a], Siwaporn Meejoo[a], I-Ming Tang[b,*]

[a] Dapartment of Chemistry, Mahidol University, Bangkok 10400, Thailand
[b] Department of Physics and Capability Building Unit in Nanoscience and Nanotechnology, Faculty of Science, Mahidol University, 10400, Thailand

ARTICLE INFO

Article history:
Received 29 February 2008
Received in revised form 22 May 2008
Accepted 30 May 2008

Keywords:
Biomaterials
Organic templating
Microstructure

ABSTRACT

Biomimetic mineralization is a method to form natural materials. We have synthesized hydroxyapatite (HAP) by using an organic template of polyvinyl alcohol (PVA) and sodium dodecyl sulfate (SDS) as the surfactant. The X-ray diffractometer (XRD) patterns show the sizes of the HAP particles to be in the nanosize (15–30 nm) range. The chemical functional groups of the HAP were investigated by Fourier transform infrared (FT-IR) which shows the formation of the hydroxyl group $(OH)^{-1}$ and the phosphate group $(PO_4)^{-3}$. The transmission electron microscopy (TEM) images show the particles to be in the range of 20–30 nm. The SDS looks like globular sphere, while the crystals of the HAP in the SDS/PVA appear as polyhedron crystal. The average size of each globular sphere is about 3–5 μm. As-prepared HAP samples were studied for their bioactive property by immersing them in a stimulated body fluid (SBF). After soaking them in SBF for one week, the SEM images show the accumulation of calcium carbonate or calcium phosphate SBF on surface of the HAP. This indicates that there might be an increased bioactive activity on the surface of the HAP prepared by this method.

© 2008 Published by Elsevier B.V.

1. Introduction

Hydroxyapatite (HAP), whose chemical formula is $Ca_{10}(PO_4)_6(HO)_2$, is very similar to the materials forming the bones in the human body. In addition to providing the structural support for the body, the bones also serve as the major reservoirs for the calcium and phosphate ions needed for various metabolic functions [1–4]. The calcium phosphates have, in general, excellent biocompatibility with the human body and integrate well into the bones upon implantation. The nanoparticles made with hydroxyapatite offer a favorable environment for protein adhesion and osteoblast proliferation [3,5,6]. The strong interfacial adhesion between the inorganic fillers [7] and the organic polymer matrix [6,8–14] is the key to creating composites having good mechanical properties. In an attempt to improve the interfacial adhesion, the surfaces of HAP nanocrytals have been modified with a diverse class of coupling agents and polymers through chemical reaction with the hydroxyl groups on the HAP surface. These materials have some disadvantages when used in tissue engineering applications such as the lack of degradability in a biological environment. They are also brittle and their capabilities for being able to be processed into a predesigned porous structure are limited. Polymeric capsulation has recently been proposed as a novel method for nanoengineering manufacturing [3,4,8–16,19].

Although the effects of uncharged polymers, of anionic surfactants, and of the polymer–surfactant mixtures on the crystallization processes of inorganic crystals have been investigated, the uses of aqueous systems containing polymer–surfactant mixture in the crystallization and aggregation of calcium phosphate have not investigated. In this work we use PVP–sodium dodecyl sulfate (SDS) solutions as the crystallization media for the synthesis of HAP. Our reason for proposing this route is that the SDS polar group through their electrostatic interaction with the calcium ions can act as the active sites for the HAP nucleation [15,16]. When the surfactants simultaneously combine with the polymer chains through their hydrophobic interaction, the aggregation states of the polymer/surfactant supramolecules will be able to control the size, shape, morphology, and poly dispersivity of HAP crystals. Part of the polyvinyl alcohol (PVA) is a hydrophilic biocompatible polymer having the various characteristics needed for biomedical applications [3,12–14]. Aqueous PVA solutions can be transformed into a solid hydro gels by the physical cross linking occurring during a freeze–thaw cycle. The PVP dispersion capability for the solid particles, as well as the mechanical stirring, prevents the direct precipitation of HAP. This favors the nucleation, growth, transformation or aggregation of HAP crystalline

* Corresponding author. Tel.: +662 201 5758; fax: +662 354 7159.
E-mail address: scimt@mahidol.ac.th (I.-M. Tang).

0254-0584/$ – see front matter © 2008 Published by Elsevier B.V.
doi:10.1016/j.matchemphys.2008.05.082

Please cite this article in press as: W. Pon-On, et al., Formation of hydroxyapatite crystallites using organic template of polyvinyl alcohol (PVA) and sodium dodecyl sulfate (SDS), Mater. Chem. Phys. (2008), doi:10.1016/j.matchemphys.2008.05.082

particles on the surfaces of PVA/SDS aggregates. However, the structural relationship between the PVA/SDS supramolecules and the inorganic minerals is too ambiguous to be widely applied to the biomimetic syntheses of functionally composite materials. Biometric synthesis involves the crystallization and aggregation processes of inorganic minerals. This synthesis is the subject of the present paper.

In this work, hydroxyapatite (HAP) has been synthesized in SDS, through the mixing the PVA with the de-ionized water (in an amount 5–25 ml). This is then followed by its mixing with the SDS. The negative charges on the SDS polar groups act as the active site for the opposite charge of Ca^{2+} to form the micelles. The formation of the HAP structure occurs as the Ca^{2+} and PO_4^{3-} ions defuse into the micelle. The rate of crystal growth depends on

Table 1
Starting chemical amounts for the preparation of the crystal structure hydroxyapatite (HAP) in the sodium dodecyl sulfate (SDS) SDS/PVA@*x* ml (H_2O), *x* = 5–25 ml

Sample	$Ca(NO_3)_2{\cdot}4H_2O$	$(NH_4)_2HPO_4$	SDS (0.001 M) (ml)	Polyvinyl alcohol (PVA)@(H_2O)
HAp_SDS	2.9802 g/10 ml/H_2O	1 g/10 ml (H_2O)	3	0
HAp_PVA5	2.9802 g/10 ml/H_2O	1 g/10 ml (H_2O)	3	0.1 g/5 ml (H_2O)
HAp_PVA10	2.9802 g/10 ml/H_2O	1 g/10 ml (H_2O)	3	0.1 g/10 ml (H_2O)
HAp_PVA15	2.9802 g/10 ml/H_2O	1 g/10 ml (H_2O)	3	0.1 g/15 ml (H_2O)
HAp_PVA20	2.9802 g/10 ml/H_2O	1 g/10 ml (H_2O)	3	0.1 g/20 ml (H_2O)
HAp_PVA25	2.9802 g/10 ml/H_2O	1 g/10 ml (H_2O)	3	0.1 g/25 ml (H_2O)

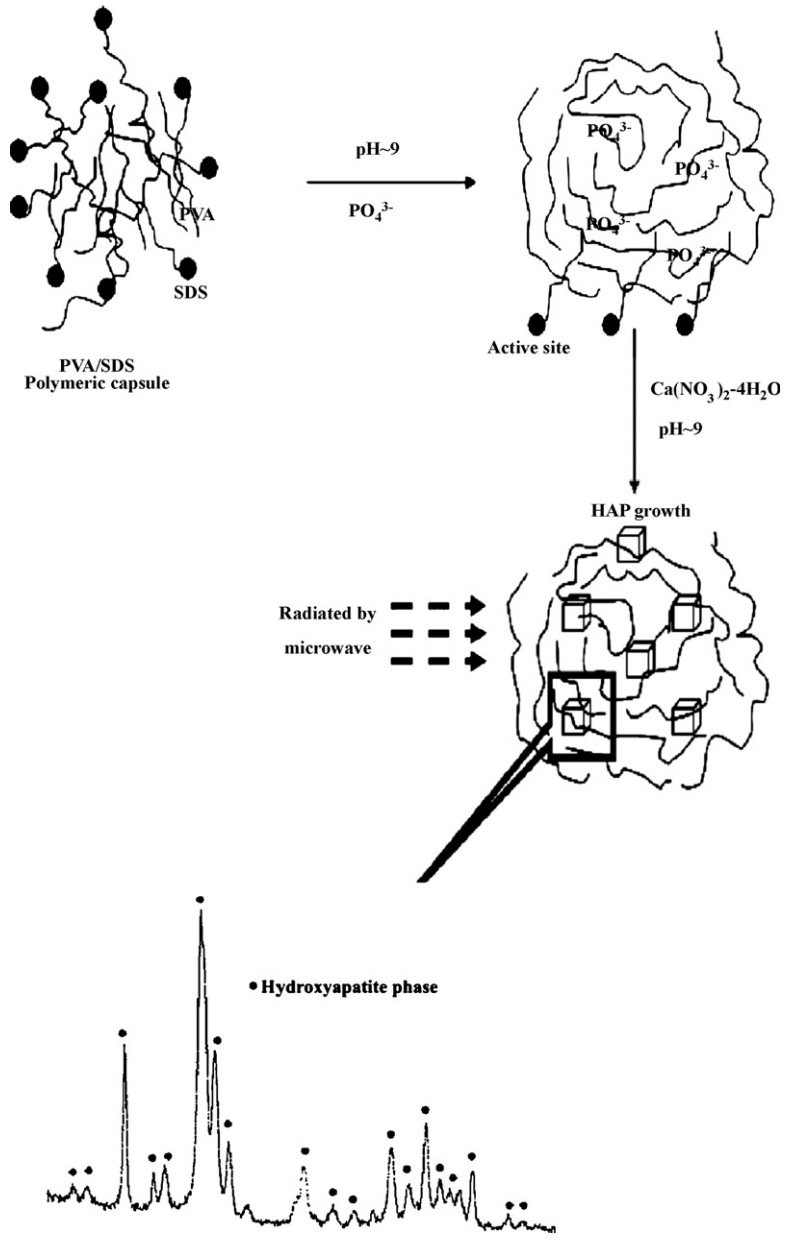

Fig. 1. Schematic of the synthesis of hydroxyapatite inside a polymeric capsule created by mixing poly vinyl alcohol (PVA) with SDS and the subsequent radiation of the capsule. The XRD pattern is that of the hydroxyapatite formed by the microwave irradiation.

Please cite this article in press as: W. Pon-On, et al., Formation of hydroxyapatite crystallites using organic template of polyvinyl alcohol (PVA) and sodium dodecyl sulfate (SDS), Mater. Chem. Phys. (2008), doi:10.1016/j.matchemphys.2008.05.082

the ratio of PVA and H_2O. This ratio is a major factor in the HAP formation.

2. Experimental details

The materials for the preparation of the hydroxyapatite are obtained by irradiating the aqueous solutions with microwaves. The starting reagents are $Ca(NO_3)_2{\cdot}4H_2O$, $(NH_4)_2HPO_4$, PVA, SDS, and $(NH_4)OH$. The amounts of calcium phosphate ($Ca(NO_3)_2{\cdot}4H_2O$), $(NH_4)_2HPO_4$, SDS and PVA in the different mixtures are listed in Table 1.

The process leading to the formation of the nanocrystallite hydroxyapatite (HAp) is shown in Fig. 1.

The details of the process are:

(i) 0.1 g of PVA is dissolved in various amounts of de-ionized water (5–25 ml) and mixed with 3 ml of SDS (0.001 M) (the sample being stirred for several time until the PVA is completely dissolved in the de-ionized water) Notably, during the stirring, bubbles occur between the interface of air and liquid.
(ii) The pH of solution is adjusted to 9 with $(NH_4)OH$ before the 10 ml of the $(NH_4)_2HPO_4$ solution is dropped into the solution which is constantly being stirred.
(iii) In this stage, the PO_4^{3-} ions are entrapped inside the polymer capsule. The formation of hydroxyapatite nanocrystals begins to appear after the 10 ml of the $Ca(NO_3)_2{\cdot}4H_2O$ solution is added to solution containing the PO_4^{3-}/polymer matrix.
(iv) After the reaction is finished, the mixture is stirred for several minutes and the pH is readjusted again to 9.0.
(v) The aqueous mixture is now put into a household microwave oven operating in the frequency bands centered at 915 MHz. The mixture is exposed to the radiation for 30 s. in an ambient atmosphere. The microwave accelerated the formation of the hydroxyapatite [18,21].
(vi) After cooling to room temperature, the precipitates (white powder) are washed several times with de-ionized water and the HAP samples are extracted by freeze drying.

The crystal structure of the sample is determined by a Bruker diffractometer (Model D8 Advance) using the Cu Kα radiation. The diffractometer is operated at 40 kV with 40 mA current. The XRD pattern is scanned over the range $2\theta = 20–60^\circ$ at a scanning speed of $0.037^\circ\ min^{-1}$. For the FT-IR measurements, the powders were mixed with KBr and pressed into pellets. These were analyzed using a FT-IR spectrometer (Spectrum GX, Perkin Elmer, USA). A scanning electron microscope (JEOL model JSM-6301F) is used to observe the changes in the sizes and in the morphology of the samples heat treated at different temperatures. An accelerating voltage of 15 kV is used to obtain the SEM images. The nanoparticles are examined by a transmission electron microscope (TEM) (TECNAI, T20).

3. Bioactivity in simulated body fluid (SBF)

To study the bioactive behavior of biomaterials, the materials are soaked in a simulated body fluid (SBF). This is a fluid which has an ionic composition very similar to that of human plasma [1,22]. The SBF solution we used is one of the more extensively used one. It contains the following amounts of chemicals: NaCl (136.8 mM), $NaHCO_3$ (4.2 mM), KCl (3.0 mM), K_2HPO_4 (1.0 mM), $MgCl_2{\cdot}6H_2O$ (1.5 mM), $CaCl_2$ (2.5 mM) and $NaSO_4$ (0.5 mM). These chemicals are mixed together and its pH is then adjusted to ~7.4. The bioactivity of HAP samples for various amounts of PVA@H_2O concentration is assessed by immersing the powders of each samples in 50 ml of SBF for 3 h, for one day and for one week at 37 °C under static condi-

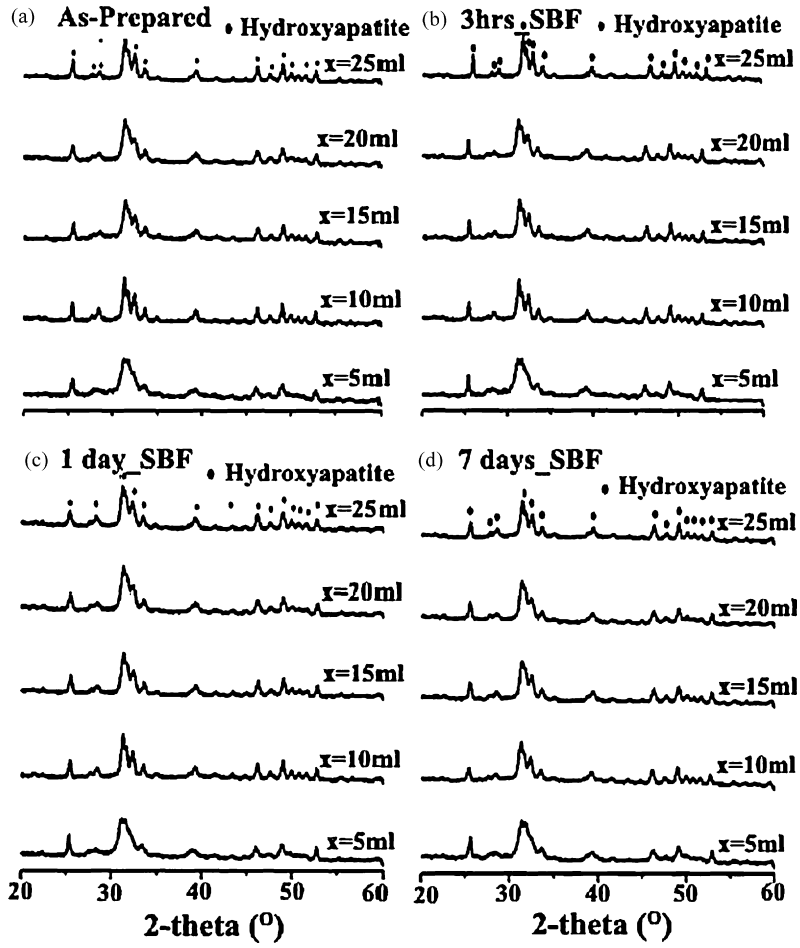

Fig. 2. XRD patterns of hydroxyapatite synthesized in SDS/0.1 g PVA_*x* ml (H_2O) where $x = 5–25$ ml. (a) The XRD patterns of an as-prepared HAP; (b) the pattern after soaking the pellets in the SBF solution for 3 h; (c) for 1 day and (d) for 1 week.

Please cite this article in press as: W. Pon-On, et al., Formation of hydroxyapatite crystallites using organic template of polyvinyl alcohol (PVA) and sodium dodecyl sulfate (SDS), Mater. Chem. Phys. (2008), doi:10.1016/j.matchemphys.2008.05.082

tions. The SBF is replaced every three days to avoid any changes in the cationic concentration that may occur due to the degradation of the samples. After immersion in the SBF, the powder samples are washed with de-ionized water before analysis with the scanning electron microscopy (SEM) and the X-ray powder diffraction (XRD).

4. Results and discussions

4.1. XRD result

The XRD patterns for the powders synthesized in solutions having different concentration of PVA in de-ionized water are shown in Fig. 2. The as-prepared powders is first washed with water several times to remove any un reacted chemicals and then they are immersed in the stimulated body fluid (SBF) for the periods mentioned above at a temperature of 37 °C. The XRD patterns of most samples show the presence of a single phase having the hydroxyapatite (HAP) structure. The sample synthesized in the solution having 0.1 g PVA dissolved in 5 ml H_2O however shows a broad pattern at 2θ about 30–35°. This broadening is due to the slower growth of HAP which occurs when the concentration of PVA gel (~0.0022 M) is high. The reaction between the calcium Ca^{2+} ions and the phosphate ions is quicker when the ions can diffuse more rapidly through the PVA gel. This is the case when the gel contains more water, i.e., the ratio PVA/H_2O is low. Evidence of this is the appearance of sharp peaks in the XRD when the PVA is dissolved in 10–25 ml of H_2O.

Fig. 2 also shows that there is no change in the XRD patterns when the powders are soaked in the SBF for longer periods (i.e., there are no changes in the patterns). This is evidence that the ions in the SBF solution did not destroy the crystal structure of the hydroxyapatite when they are surrounded by the SBF for less than one week. The average crystallite sizes can be calculated from Shearer's formula [5,20], using the half width of the [0 0 2] peak at $2\theta \sim 26°$. The average crystallites sizes are between 15–30 nm. A plot of the average sizes of the nanoparticles formed in solutions containing 0.1 g PVA dissolved in different amounts of H_2O is shown in Fig. 3.

4.2. FT-IR results

The FT-IR spectrum analyses of the as-prepared HAP precipitated in SDS and of the PAP precipitated in the different concentrations of PVA/SDS gel and which were soaked for one week in the SBF are shown in Fig. 4(a) and (b), respectively. The dominant bands seen in the FT-IR spectrums of the as-prepared HAP are due to the presence of two types of carbonate–hydroxyapatite bonds in

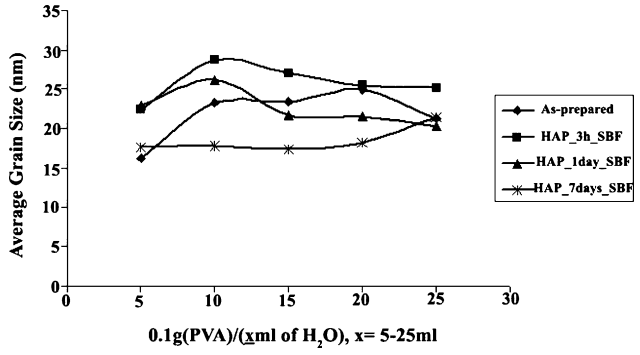

Fig. 3. Average particle size the nanoparticles synthesized when the SDS is added is solutions of 0.1 g of PVA and different amount of HO_2.

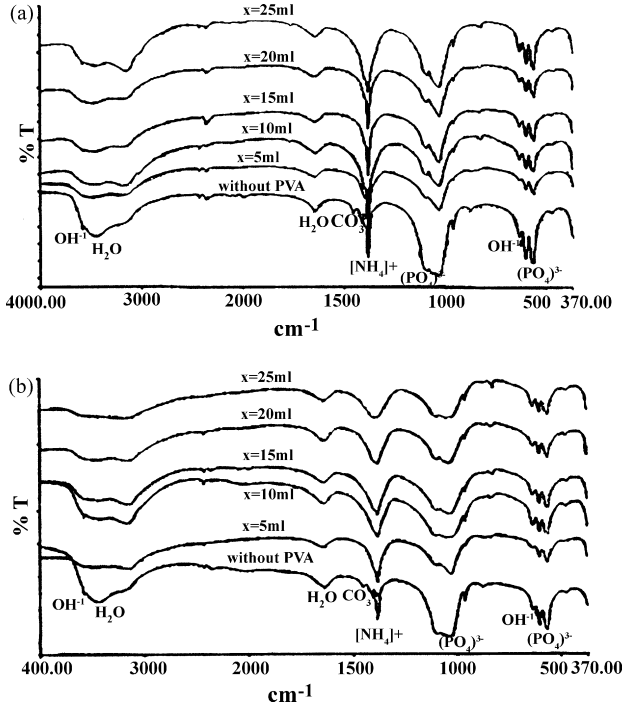

Fig. 4. FT-IR spectra of synthesized hydroxyapatite. The curves show the signals arising from the chemical residues on the powder after they were precipitated. (a) The signals from an as-prepared hydroxyapatite pellets. (b) The signals after the pellets were soaked in the SBF fluid.

the HAP's. The stretching and vibrating modes of hydroxyl group appear at about 3575 and 627 cm^{-1}, respectively. The intensity of the stretching mode of the hydroxyl (OH^{-1}) group in the spectra for HAP synthesized in the presence of SDS only is very weak. This mode can not be seen in the spectra for the sample synthesized in the presence of both SDS/PVA since the 3575 cm^{-1} peak is strongly overlapped by the broad H_2O band which occurs at 3415 cm^{-1}.

The changes which occur when different PVA/H_2O ratios are used are similar to those seen in the samples prepared in pure SDS except for the presence of the carbonate peaks. The presence of a small amount of $CO_3{}^{-2}$ groups is reflected by the appearances of peaks in the range between 1459–1411 cm^{-1} and at 876 cm^{-1} [8,17,24,25]. The intensities of these peaks are very low. The broad bands observed at 3416 and 1637 cm^{-1} [8,17,23,26] are due to the absorbed water on the surface on the HAP crystallites. The intense bands seen at 1088, 1035 and 961 cm^{-1} are due to the $(PO_4)^{-3}$ stretching modes [8,24]. The doublet at 602 and 562 cm^{-1} are due to the $(PO_4)^{-3}$ blending mode [8,23,26]. Finally the peak at 1383 cm^{-1} is due to the $[NH_4]^+$ group. This peak disappears when the samples are heated to 500 °C for 2 h.

From the FT-IR spectrums of the samples soaked in SBF and kept at 37 °C for 7 days (see Fig. 4(b)), we conclude that the chemical bonds which produce the FT-IR spectra seen in the hydroxyapatite synthesized without and with the different PVA concentration (0.1 g PVA@x ml H_2O; x = 5, 10, 15, 20 and 25 ml) are almost the same as bonds present before the powders were soaked in the SBF solution. The FT-IR bands for the OH^{-1}, $CO_3{}^{-2}$, $(PO_4)^{-3}$ groups as well as those for the H_2O are present. Comparing the spectra for the samples soaked in SBF at 37 °C for one week and that of the as-prepared powder, we see that the intensity of the O—H stretching mode increase as the amount of de ionized water used was increased from 10 to 15 ml. The main observation is the appearance of the band for the $CO_3{}^{-2}$ group vibration at 876 cm^{-1}. The broadening of the FT-IR bands of spectra seen at 1088, 1035 and 961 cm^{-1}

Please cite this article in press as: W. Pon-On, et al., Formation of hydroxyapatite crystallites using organic template of polyvinyl alcohol (PVA) and sodium dodecyl sulfate (SDS), Mater. Chem. Phys. (2008), doi:10.1016/j.matchemphys.2008.05.082

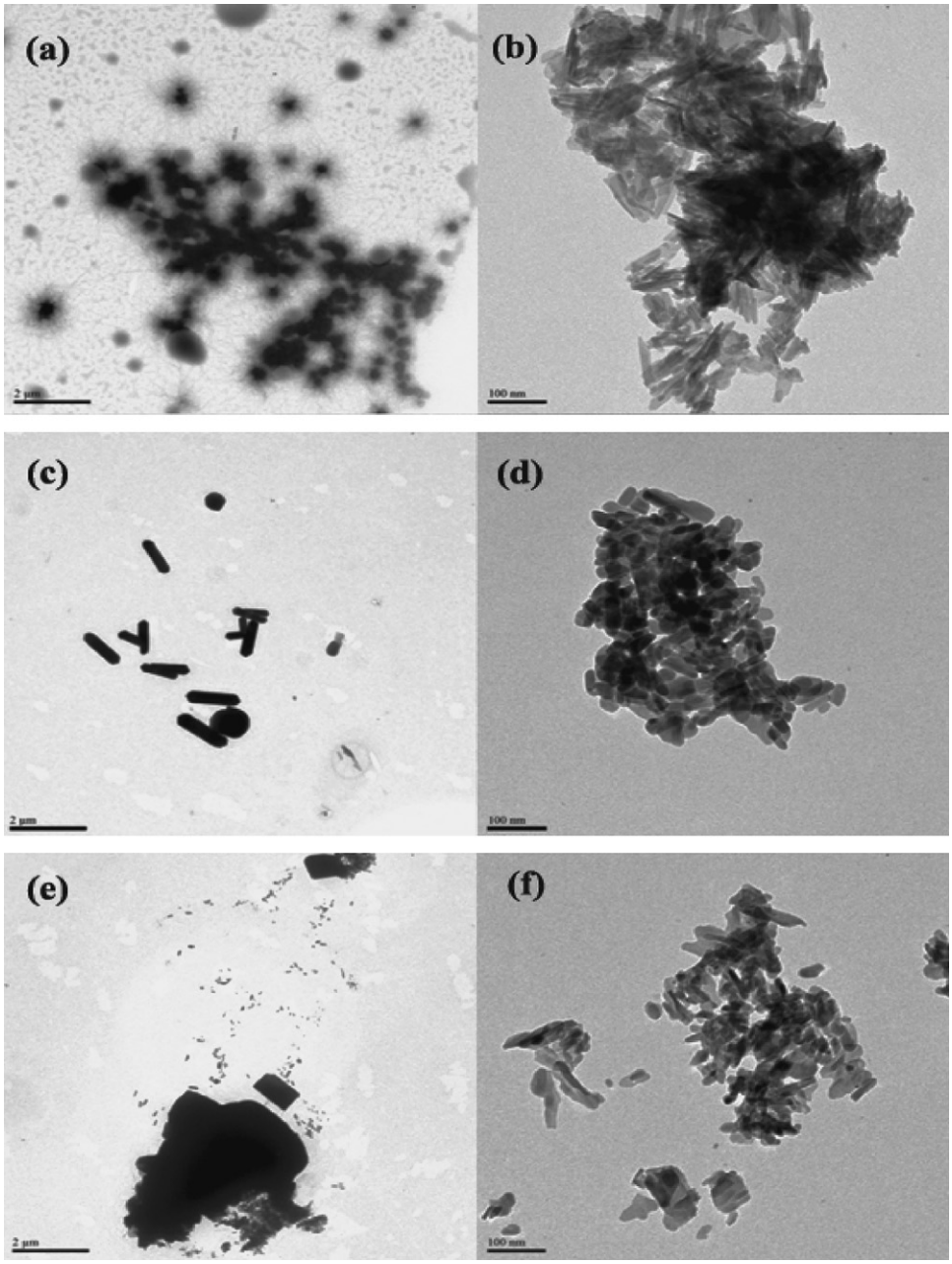

Fig. 5. Low-magnification TEM (left side frames) and high magnification (right-hand frames) of hydroxyapatite nanostructure. (a) Low magnification image; (b) low field magnification of HAP synthesized in SDS; (c–f) TEM of hydroxyapatite in the presence of SDS/0.1 g PVA in 5 and 25 ml H_2O, respectively.

is most likely due to the changes in the $(PO_4)^{-3}$ stretching modes resulting from the distortion of the HAP crystalline structure occurring when the $CO_3{}^{-2}$ ions replace the phosphate groups in the HAP structure. When this happens, we have a B-type hydroxyapatite. The presence of the ions in the SBF solution also causes the HAP to be poorly crystallized. This would weaken the Ca—P bonds in the HAP structure.

4.3. TEM result

Fig. 5 shows the TEM images of the nanocrystals The shapes and crystallite sizes of the HAP synthesized with SDS present are seen Fig. 5(a) and (b). Fig. 5(c) and (f) shows the shapes and sizes of crystallites formed when the HAP was synthesized in the solutions of SDS/0.1 g (PVA) dissolved in different amounts of water. The images shown in Fig. 5(a) are those taken at the highest magnification used in this study and are of the as-prepared formation of the HAP in SDS. The images show that the shapes of particles are star like. The center of star is made of the HAP, while the branch may be from the micelle surfactant. The sizes of stars are controlled by the shape and size of the HAP particles. Fig. 5(b) shows the nanoribbons structure of the HAP in the SDS solution. The pictures of the ribbons were obtained after washing the capsules several times to remove the SDS. The sizes of ribbons are about 10–20 nm in width and 50–100 nm in length. The shapes of HAP crystallites grown in the presence SDS/PVA at various concentrations of the H_2O (see Fig. 5(c) and (f))) are (nano) rod-like, needle-like, circular and rectangular. These shapes may be due to the shape of

Please cite this article in press as: W. Pon-On, et al., Formation of hydroxyapatite crystallites using organic template of polyvinyl alcohol (PVA) and sodium dodecyl sulfate (SDS), Mater. Chem. Phys. (2008), doi:10.1016/j.matchemphys.2008.05.082

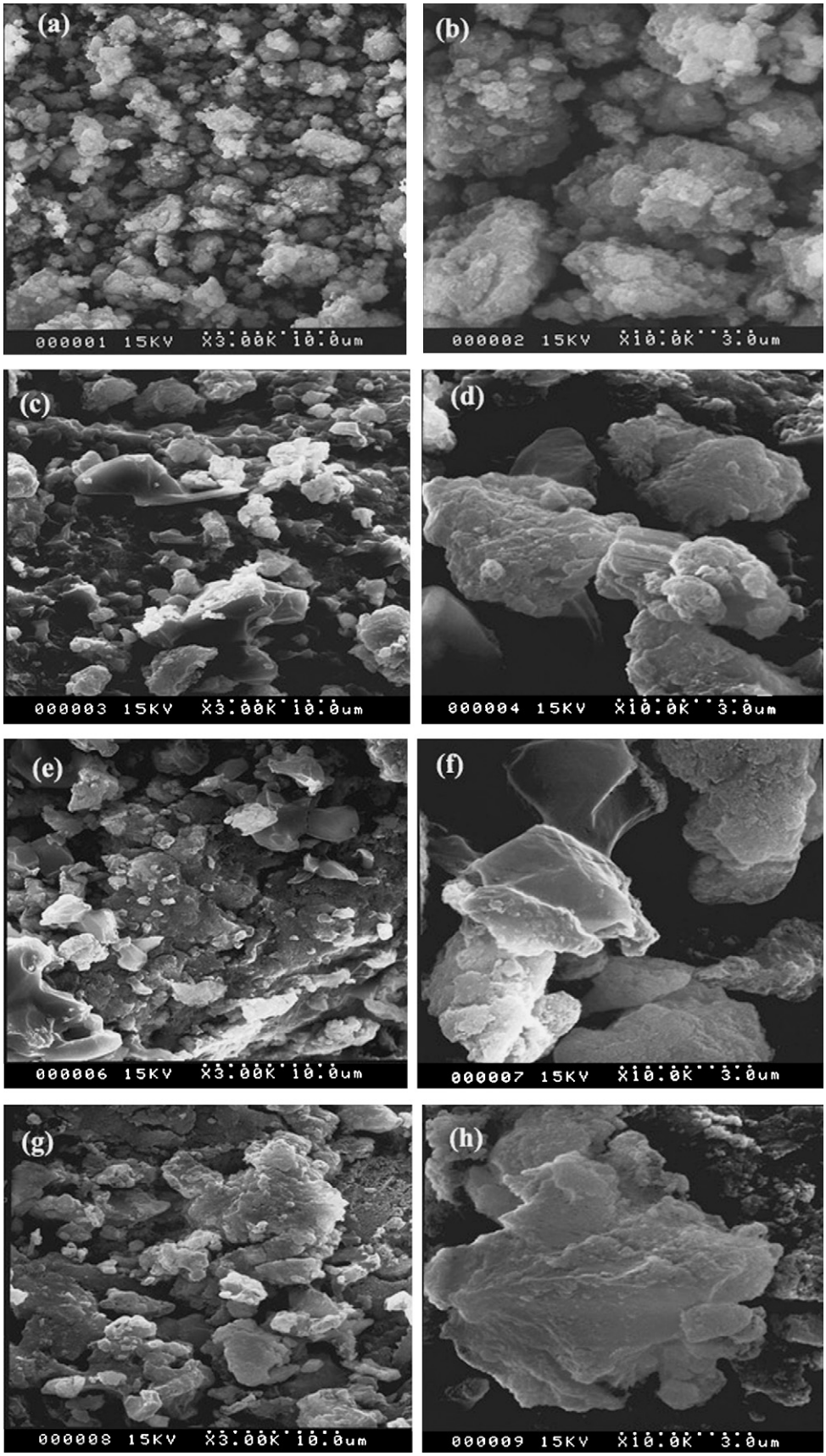

Fig. 6. SEM images. The images show the changes in the hydroxyapatite structure (a) in the presence of only SDS; (b) in the presence of SDS/0.1 g PVA with 5 ml (H_2O) (c and d), SDS/0.1 g PVA_15 ml (H_2O) (e and f) and SDS/0.1 g PVA_5 ml (H_2O) (g and h).

Please cite this article in press as: W. Pon-On, et al., Formation of hydroxyapatite crystallites using organic template of polyvinyl alcohol (PVA) and sodium dodecyl sulfate (SDS), Mater. Chem. Phys. (2008), doi:10.1016/j.matchemphys.2008.05.082

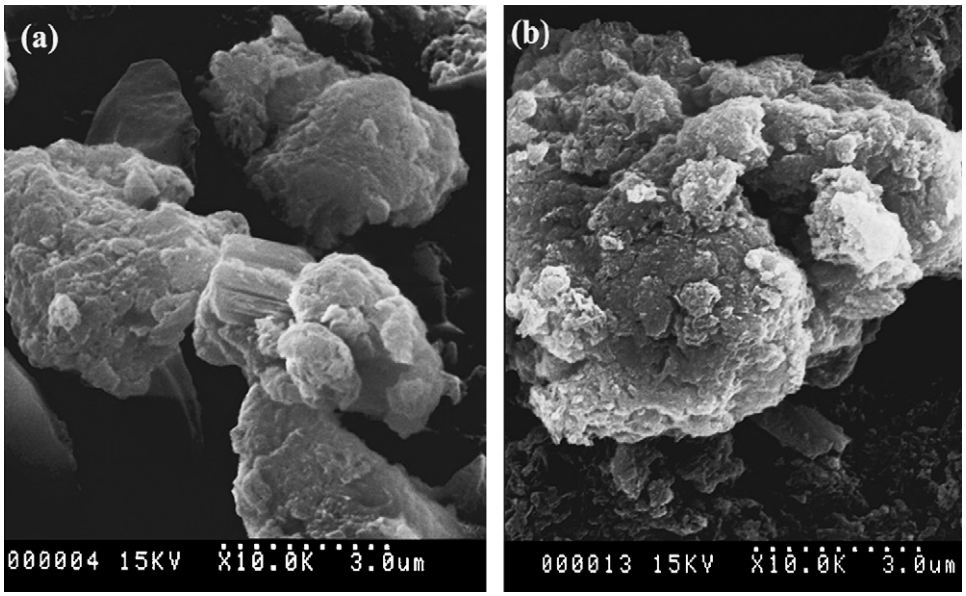

Fig. 7. SEM images. Images of the synthesized hydroxyapatite synthesized in the presence of SDS. But before they were soaked in SBF (a) before they were soaked in SDS; (b) after they were soaked in stimulated body fluid (SBF) at 37 °C for 1 week.

template, i.e., the supramolecule formed by the PVA polymer and surfactant.

The needle-like HAP crystallites are formed when the template has a cylindrical structure. This happens when the negative charge on the SDS of the SDS acts as the active site for the Ca ions. The calcium ions can then react with the phosphate groups within the cylindrical capsule and form needle shape. The size of needle depends on rate of diffusion of the reactant ions through the PVA gel.

4.4. SEM result

The low and high magnification SEM micrographs of the HAP particles are seen in Fig. 5. The images seen in Fig. 6(a) and (b) are the aggregations of the HAP particles precipitated from the solution of pure SDS. The images seen in Fig. 6(c)–(h) are of the HAP particles precipitated from solutions of 0.1 g PVA dissolved in 5, 15 and 25 ml of de ionized water, respectively. The HAP particles prepared in the SDS only appear as spherical particles. The particles prepared in the PVA/SDS solutions are in the shape of polyhedron crystal. These are less porous than those synthesized in SDS only. The averages sizes of the particles synthesize in the presence of PVA and SDS are in the range of 3–5 μm. This shows that template having the PVA/SDS produces different results. The reasons for this is that the sulfate groups belonging to the SDS in the template having the PVA/SDS can also act as an active site. This would cause the HAP particles to grow in an irregular manner.

4.5. Hydroxyapatite in simulated body fluid (SBF)

The effects of soaking the hydroxyapatite in the simulated body fluid are seen in the SEM micrograms appearing in Fig. 7. The HAP particles seen here are synthesized from SDS/0.1 g PVA in 5 ml de ionized water. The two micrograms show the HAP before and after they were soaked in SBF for 1 week. As we see, the surface of HAP has changed, i.e., it has become much rougher. We attribute this roughness to the accumulation of calcium carbonate (or calcium phosphate) on the surface. This interpretation is supported by the FT-IR measurements which show the appearance of the $CO_3{}^{-2}$ group vibration band at 876 cm^{-1}. This interpretation is also supported by the increase in the intensities of the XRD peak at $2\theta \sim 35^\circ$ and the splitting of the peak at $2\theta \sim 26^\circ$ in the HAP powders soaked in the SBF (Fig. 1(b)–(d)). We lump the HAP particles which have a surface roughness as being part of a new apatite-like phase. Expecting the same will occur under *in vivo* conditions; this new apatite-like phase should form on the surface of the hydroxyapatite after its implantation into the body.

Acknowledgement

We would like to thank the Center for innovation in Chemistry: Postgraduate Education and Research in Chemistry (PERCH-CIC) Program, Mahidol University for full financial support. SM and IMT would like to thank the The Thailand Research Fund (TRF) for partial support under the grants MRG5080059 and BRG51, respectively.

References

[1] M. Vallet-Regí, J. Chem. Soc., Dalton Trans. (2001) 97.
[2] M. Sato, T.J. Webster, Expert Rev. Med. Dev. 1 (2004) 105.
[3] R. Murugan, S. Ramakrishna, Compos. Sci. Technol. 65 (2005) 2385.
[4] L.A. Estroff, L. Addadi, S. Weiner, A.D. Hamilton, Org. Biomol. Chem. 2 (2004) 137.
[5] A. Ogose, T. Hotta, H. Kawashima, N. Kondo, W. Gu, T. Kamura, N. Endo, J. Biomed. Mater. Res. Part B: Appl. Biomater. 72N (2005) 94.
[6] K. Mi Woo, J. Seo, R. Zhang, P.X. Ma, Biomaterials 28 (2007) 2622.
[7] V.M. Rusa, C.H. Ng, M. Wilke, B. Tiersch, P. Fratzl, M.G. Peter, Biomaterials 26 (2005) 5414.
[8] M.G. Ma, Y.J. Zhu, J. Chang, J. Phys. Chem. B 110 (2006) 14226.
[9] D.G. Shchukin, G.B. Sukhorukov, H. Möhwald, Chem. Mater. 15 (2003) 3947.
[10] R. Joseph, K.E. Tanner, Biomacromolecules 6 (2005) 1021.
[11] J. Watanabe, M. Akashi, Biomacromolecules 7 (2006) 3008.
[12] A. Sinha, G. Das, B.K. Sharma, R.P. Roy, A.K. Pramanick, S. Nayar, Mater. Sci. Eng. C 27 (2007) 70.
[13] L.E. Millon, H. Mohammadi, W.K. Wan, J. Biomed. Mater. Res. Part B: Appl. Biomater. 79B (2006) 305.
[14] T. Kaneko, D. Ogomi, R. Mitsugi, T. Serizawa, M. Akashi, Chem. Mater. 16 (2004) 5596.
[15] M. Bujan, M. Sikirić-Vinceković, N. Vdović, N. Garti, H. Füredi-Milhofer, Langmuir 17 (2001) 6461.
[16] G.K. Lim, J. Wang, S.C. Ng, L.M. Gan, Langmuir. 15 (1999) 7472.
[17] S. Zhou, X. Zheng, X. Yu, J. Wang, J. Weng, X. Li, B. Feng, M. Yin, Chem. Mater. 19 (2007) 247.

Please cite this article in press as: W. Pon-On, et al., Formation of hydroxyapatite crystallites using organic template of polyvinyl alcohol (PVA) and sodium dodecyl sulfate (SDS), Mater. Chem. Phys. (2008), doi:10.1016/j.matchemphys.2008.05.082

[18] Z. Zhang, D. Gao, H. Zhao, C. Xie, G. Guan, D. Wang, S.H. Yu, J. Phys. Chem. B 110 (2006) 8613.
[19] S. Thachepan, M. Li, S.A. Davis, S. Mann, Chem. Mater. 18 (2006) 3557.
[20] N.Y. Mostafa, Mater. Chem. Phys. 94 (2005) 333.
[21] J. Liu, K. Li, H. Wang, M. Zhu, H. Xu, H. Yan, Nanotechnology 16 (2005) 82.
[22] S. Jalota, A.C. Tas, S.B. Bhaduri, J. Am. Ceram. Soc. 88 (12) (1995) 3353.
[23] S. Koutsopoulos, J. Biomed. Mater. Res. 62 (2002) 600.
[24] S. Pushpakanth, B. Srinivasan, B. Sreedhar, T.P. Sastry, Mater. Chem. Phys. 107 (2008) 493.
[25] J.D. Chen, Y.T. Wang, K. Wei, S.H. Zhang, X.y. Shii, Biomaterials 28 (2007) 2275.
[26] Y. Wang, S. Zhang, K. Wei, N. Zhao, X. Wang, Mater. Lett. 60 (2006) 1484.

Please cite this article in press as: W. Pon-On, et al., Formation of hydroxyapatite crystallites using organic template of polyvinyl alcohol (PVA) and sodium dodecyl sulfate (SDS), Mater. Chem. Phys. (2008), doi:10.1016/j.matchemphys.2008.05.082

Advanced Materials Research Vols. 55-57 (2008) pp 689-692
online at http://www.scientific.net
© (2008) Trans Tech Publications, Switzerland
Online available since 2008/Aug/22

Substitution of Iron in Preparation of Enhanced Thermal Property and Bioactivity of Hydroxyapatite

S. Meejoo[a], W. Pon-On, S. Charnchai and T. Amornsakchai

[1]Department of Chemistry, Faculty of Science, Mahidol University,

Rama VI Rd., Rajathevi, Bangkok 10400 Thailand

[a]scsmj@mahidol.ac.th

Keywords: Hydroxyapatie, Iron, Thermal property, Bioactivity, Vickers Microhardness

Abstract. Incorporation of Iron into hydroxyapatite (HAp) has generated a novel material for which their properties differ from those of conventional HAp. Although XRD indicated that the as-prepared iron-substituted hydroxyapatite (HApFe) is of a single crystalline phase similar to that of HAp, we found that carbonate ions can incorporate in the HApFe structure 3 times better than in HAp. As results, HApFe possesses the Vickers microhardness about 1.5 times higher than that of HAp. Thermal behaviors and bioactivity of HApFe are discussed in comparison to those of HAp. Various experimental methods have been employed in this work including powder XRD, IR, SEM, DSC/TGA and Vickers Hardness testing.

Introduction

Hydroxyapatite (HAp) is well known as the major mineral component of hard tissue in bone and teeth [1-3]. There is considerable interest in dental applications and use in artificial bone substitution for surgical treatment of bone defects [4]. However, HAp has limited ability in forming an interface with new bone tissue. The natural bones in the human body provide the structural support for the body. Furthermore, they also serve as a major reservoir of calcium and phosphate ions needed for a variety of metabolic functions. Besides Ca and P, bones can serve as a major reservoir for other elements needed in a variety of metabolic processes [1]. These elements substituted in hydroxyapatite can be made biocompatible. Ability to participate in cellular functions and osteoconductivity are important biological activities of hydroxyapatite based implant materials. The effect of element substitutions in hydroxyapatite has been investigated with several elements such as Si, Na, Cu, Zn and Mg [5-12] where these experiments focused on the formation of HAp and Ca deficient hydroxyapatite. Another area of interest caused by the substitution of elements in HAp structure is whether these elements can modify its structure and enhance the bioactivity of HAp. The effect of Mg substitution on the crystallization of HAp has been reported in [2, 8, and 11] and the substitution of silicon in HAp [7-9] is also of interest. Iron is an essential element in the human metabolism and the incorporation of Fe into HAp could accomplish this task. The effect of iron on the properties of HAp has not been reported in the literature on the use of HAp as a biomaterial. The primary objective of this work is to investigate the inter-relationship among the structural, thermal, mechanical properties and bioactivity of the iron-substituted hydroxyapatite (HApFe), the material of high potential in medical applications.

Experimental

Hydroxyapatite (HAp) was prepared from an aqueous precipitation reaction using $Ca(NO_3)_2 \cdot 4H_2O$ and $(NH_4)_2HPO_4$ as Ca and P precursors respectively. The molar ratio of Ca/P is fixed at 1.67. The pH of both precursor solutions must be adjusted to 9.0 by NH_4OH before starting the reaction. Then, equivolume of $(NH_4)_2HPO_4$ aqueous solution was slowly added to the $Ca(NO_3)_2 \cdot 4H_2O$ solution where the solution were kept at pH=9.0 throughout reaction by adding NH_4OH. The mixture was kept under a constant stirring condition at room temperature. Next, the mixture was exposed to microwave radiation (850W) for 3 minutes and a white paste subsequently formed. The precipitate was washed

All rights reserved. No part of contents of this paper may be reproduced or transmitted in any form or by any means without the written permission of the publisher: Trans Tech Publications Ltd, Switzerland, www.ttp.net. (ID: 202.28.179.3-24/08/08,05:28:49)

using deionized water to achieve pH ~7. Then, the solvent was completely removed under freeze drying. Furthermore, Fe-substituted HAp was prepared using the C and P precursor mentioned above and $C_{12}H_{22}FeO_{14}$ as iron source. The molar ratio of (Ca+Fe)/P is fixed at 1.67 whereas the mol% of Fe is equal to 0.2, assuming that the Fe substitution resulted in the replacement of the Ca ion by the Fe ions. In this case, the $(NH_4)_2HPO_4$ solution of pH=9 was slowly added to the Ca+P precursor solution while the reaction mixture was kept at pH=9.0 throughout reaction using NH_4OH. Then, the mixture were exposed to microwave irradiation, washed by de-ionized water and freeze-dried as previously described. The bioactivity testing was performed using a simulated body fluid (SBF), an aqueous mixture of pH~7.4 containing multi-ions of the same types and concentrations as found in human plasma. In vitro tests were carried out by immersing the HAp and HApFe pellets in 50 ml of SBF for one week at 37 °C in static state yielding HAp/SBF and HAp/SBF samples respectively. After immersion in SBF, the sample was rinsed with deionized water before performing microstructure analyses. All powder X-ray diffractograms were recorded on a Bruker D8 Advance diffractometer, Cu $K_{\alpha 1}$ with PSD detector; 2θ range 20°-60°; step size 0.0154° and step time 1 second. IR measurements were performed on a Spectrum GX, Perkin Elmer IR spectrometer in the wave number region 400-4000 cm^{-1}. Both DSC and TGA thermograms were recorded on a DSC-TGA simultaneous thermal analyzer performing under N_2 atmosphere with a 20 °C/minute heating rate over a temperature range between 50° and 1200° C. SEM micrographs were recorded on a JEOL JSM 6301F electron microscope operating with an acceleration voltage of 15 kV. Vickers Microhardness tests were performed on a HMV-2000 Shimadzu Micro-Hardness Tester. A Vicker microindentor at a load of 1.96 N (200 gf) applied for 15 second was used during the testing according to the ASTM C 1327-99 standard procedure.

Results and Discussion

As seen in Fig. 1. powder XRD patterns of HApFe is quite similar to that of HAp which indicated that the as-prepared products are of a single crystalline phase of hydroxyapatite (XRD JCPDS data file No. 9-432). In Fig. 2, IR spectra have confirmed that both HAp and HApFe are of a B-type apatite structure, hydroxyapatie containing a fraction of carbonate ions, CO_3^{2-}, substituted at the phosphate, PO_4^{3-}, sites in the structure. The characteristic doublet peaks around 1450, 1640 and 873 cm^{-1} correspond to the vibration frequencies of carbonate ions. The relative amount of carbonate ions in HApFe is compared to that in HAp, where the $[CO_3^{2-} : PO_4^{3-}]_{HApFe}$ /$[CO_3^{2-} : PO_4^{3-}]_{HAp}$ is equal to 3:1, quantified based on the intensity of IR peaks corresponding to the CO_3^{2-} and the PO_4^{3-} at 1030 and 1420 cm^{-1} respectively. Note that from XRD and IR results, there is no evidence of any additional phase due to the incorporation of iron into the apatite structure.

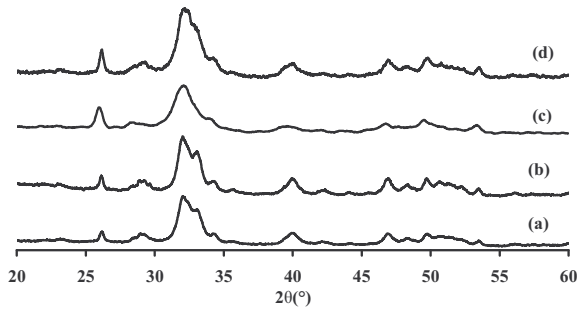

Figure 1. Powder XRD profiles of (a) HAp, (b) HAp/SBF, (c) HApFe and (d) HApFe/SBF

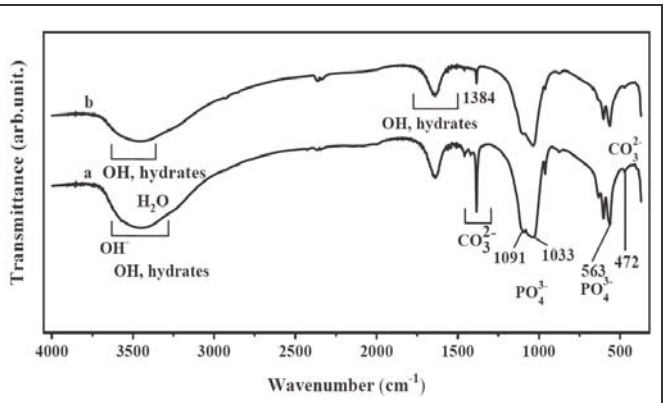

Figure 2. IR spectra of (a) HAp and (b) HApFe

From mechanical testing, the average of Vickers microhadness of HApFe is 41 HV whereas it was only 30 HV for HAp. Furthermore, Fig. 3 shows the DSC/TGA plots for HAp and HApFe and the thermal behaviors of both samples were described in Table 1.

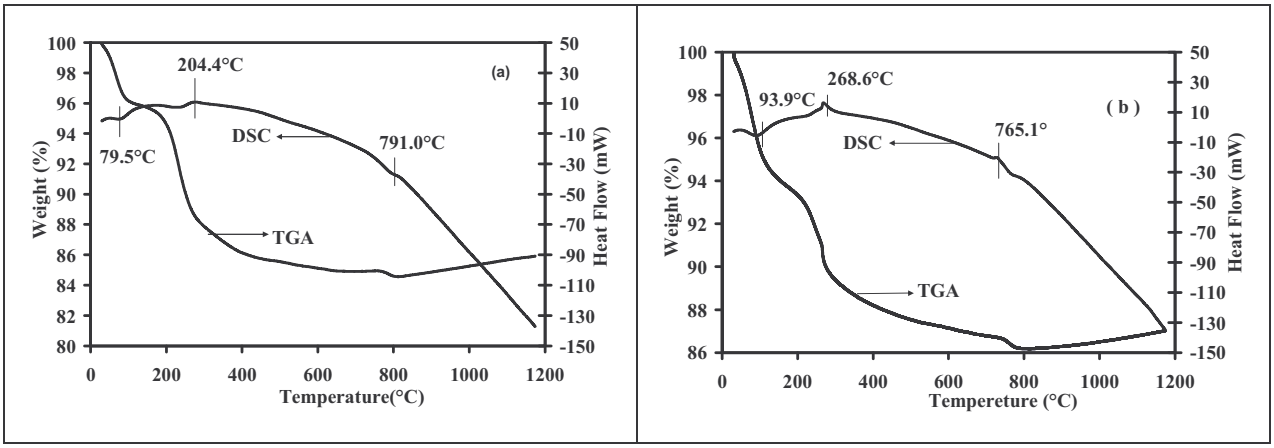

Figure 3. DSC/TGA plots of (a) HAp and (b) HApFe

Table 1. Possible assignments of the thermal events observed in DSC/TGA thermograms.

	Transition temperature / °C	Remark	Possible assignment
HAp	79.5	Endothermic	Removal of adsorbed water
	204.4	Endothermic	Removal of lattice water
	791.0	Endothermic	Decarboxylation and decomposition
HApFe	93.9	Endothermic	Removal of adsorbed water
	268.6	Exothermic	Removal of lattice water
	765.1	Endothermic	Decarboxylation and decomposition

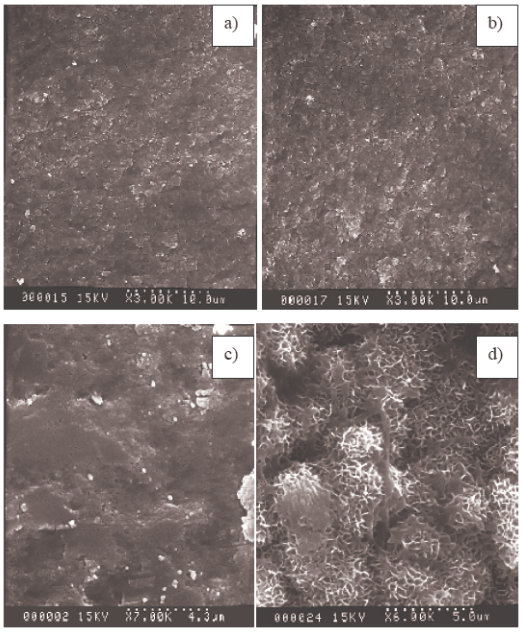

Figure 4. SEM micrographs of (a) HAp; (b) HAp/SBF;
(c) HApFe and (d) HApFe/SBF

It should be pointed out that HApFe is relatively high thermal stability comparing with that of HAp. Although the exothermic event observed from the HApFe sample is not well understood, having Fe incorporated in the apatite structure may cause the complex thermal behaviors. Figure shows SEM micrographs of the HAp and HApFe pellets after the *in vitro* bioactivity test. As seen in Fig. 4(d), the HApFe surface is evidently active with SBF after placing the apatite sample in SBF solution for one week as the nucleation and growth of hydroxyapatite substantially occurs. The microstructure of the precipitate calcium phosphate on the HApFe surface displays a sponge liked structure with irregular pores. The SEM micrographs give excellent agreement to the XRD result such that the XRD pattern of the SBF-soaked HApFe sample showed substantially increased crystalline hydroxyapatite structure. Hence, the HApFe surface enhances new HAp phase to form quicker than the HAp surface.

click for feedback
consult - comment - contact

Summary

By incorporating iron (concentration of 0.2 mol% in solution) into the precursor solutions used to synthesize HAp, we achieved an apatite material representing significantly interesting properties. HApFe represents relatively high bioactivity, mechanical property, and thermal stability in comparison to that of HAp. The higher content of CO_3^{2-} substituted at the phosphate site for HApFe may play an important role in the modified properties of this apatite material.

Acknowledgment

This work was supported by the Commission of Higher Education, Thailand Research Fund (Grant #MRG5080059) and the Center of Innovation in Chemistry: Postgraduate Education and Research Program in Chemistry (PERCH-CIC).

References

[1] S.V. Dorozhkin and M. Epple: Angew. Chem. Int. Ed., Vol.41 (2002), p. 3130.

[2] P.N. Kumta, C. Sfeir, D.H. Lee, D. Olton and D. Choi: Acta Biomater., Vol.1 (2005), p. 65.

[3] M. Vallet-Regí and J.M. González-Calbe: Prog. Solid. State., Ch.32 (2004), p. 1.

[4] H. Liu and T.J. Webster: Biomaterials., Vol.28 (2007), p. 354.

[5] Z. Yang, Y. Jiang, L.X. Yu, B. Wen, F. Li, S. Sun and T. Hou: J. Mater. Chem., Vol.15 (2005), p. 1807.

[6] D. Arcos, J. Rodríguez-Carvajal and M.Vallet-Regi: Chem. Mater., Vol.16 (2004), p. 2300.

[7] M. Vallet-Regi and D. Arcos: J. Mater. Chem., Vol.15 (2005), p. 1509.

[8] A.M. Pietak, J.W. Reid, M.J. Stuff and M. Suyer: Biomaterials., Vol.28 (2007), p. 4023.

[9] J. Li, Y. Li, L. Zhang and Y. Zuo: Appl. Surf. Sci., Vol.254 (2008), p. 2844.

[10] S.J. Kalita and H.A. Bhatt: Mater. Sci. Eng., Vol.27C (2007), p. 837.

[11] E. Landi, S. Sprio, M. Sandri, G. Celotti and A. Tampieri: Acta Biomater., Vol.4(3) 2008, p. 656.

[12] E. Landi, A. Tampieri, G. Celotti, S. Sprio, M. Sandri and G. Logroscino: Acta Biomater., Vol.3(6) 2007, p. 961.

consult
comment
contact
click for feedback

Advanced Materials Research Vols. 55-57 (2008) pp 537-540
online at http://www.scientific.net
© (2008) Trans Tech Publications, Switzerland
Online available since 2008/Aug/22

click for feedback
consult - comment - contact

Mechanochemical Treated Multi-walled Carbon Nanotubes for Incorporation of Metal Ions

U. Rinzin[1], P. Singjai[2], P. Wilairat[1] and S. Meejoo[1,a]

[1]Department of Chemistry, Faculty of Science, Mahidol University, Rama VI Rd., Rajathevi, Bangkok 10400 Thailand

[2]Department of Physics, Nanomaterials Research Unit, Faculty of Science, Chiang Mai University, Chiang Mai 53000 Thailand

[a]scsmj@mahidol.ac.th

Keywords: Multi-walled carbon nanotubes, Metal ions, Meachanochemical treatment

Abstract. Ni catalyst was removed from as received multi-walled Carbon Nanotubes (MWNTs) by acid treatment. Then, the nanotubes were treated with 4M HCl during a ball milling processing yielding mechanochemical treated MWNTs (mech-MWNTs). TEM micrographs indicate that the mech-MWNTs were still of a tubular form but with much shorter length. The equilibrium adsorption of metal ions, e.g Cu^{2+} and Ni^{2+}, on the mech-MWNTs was investigated at room temperature. The adsorption isotherms gave excellent consistence with the Langmuir theory and the ***best fit*** values of K^{-1} and N_{max} can be evaluated using non-linear least-squares. As results, the maximum of Cu^{2+} and Ni^{2+} ions uptake on to the mech-MWNTs are 0.93 ± 0.004 mg/g and 2.11 ± 0.01 mg/g respectively. There is no evidence indicating that the pore structure and layer surfaces at both ends of the mech-MWNTs are appropriate sites for metal ions adsorption.

Introduction

Carbon nanotubes (CNTs), a new form of carbon, have attracted much attention and stimulated extensive research activities across the world since its discovery in 1991 by Sumio Iijima [1]. Their unique chemical and physical properties show a great potential for wide applications such as using for polymer composite [2], field emissions [3], energy storage [4] and sensor [5]. One of the most important properties of CNTs is the relatively large specific surface area, which enables them to become candidate for adsorption of gases [6], metal ions [7,8] and organic compounds [9,10]. The large adsorption capacity of CNTs is mainly attributed to their pore structure, surface area and the existence of various types of surface functional groups. The primary objective of this research is to explore the adsorption capability of multi-walled carbon nanotubes (MWNT) to some metal ions, e.g. Cu^{2+} and Ni^{2+}. Particular emphasis is placed on understanding the surface properties in terms of selectivity and adsorption capacity of metal ions of the nanostructured materials in an isothermal adsorption process. In this work, the structure and adsorption behaviors of as received MWNTs have been investigated in comparison to those of catalyst free MWNTs, denoted as cf-MWNTs, and mechanochemical treated MWNTs, denoted as mech-MWNTs. Various experimental techniques have been employed, including powder X-ray diffraction, tranmission electron microscopy and flame atomic absorption spectroscopy.

Experimental

As-received MWNTs has been supplied from the Nanomaterials Research Unit, Chiang Mai University. This material was synthesized by an alcohol infusion method using nickel (Ni) as catalyst [11]. In order to remove Ni from the tabular nanostructure, the as-received sample was soaked in 4 M HCl aqueous solution, kept under a constantly stirring condition at room temperature for 3 hours and then washed thoroughly with deionized water to achieve pH ~7. Subsequently, the nanomaterial was dried at 80 °C obtaining the cf-MWNTs. Furthermore, the mech-MWNTs were prepared by ball

consult comment contact
click for feedback

All rights reserved. No part of contents of this paper may be reproduced or transmitted in any form or by any means without the written permission of the publisher: Trans Tech Publications Ltd, Switzerland, www.ttp.net. (ID: 202.28.179.3-24/08/08,05:28:35)

milling the as-received MWNTs in a 4 M HCl aqueous solution for 24 hours using zirconia balls (Y_2O_3-ZrO_2). Then, the mixture was washed thoroughly with deionized water to achieve pH ~7 and subsequently dried at 80 °C. To perform the metal ions adsorption experiment, 20 mg of the carbon materials was placed for 5 minutes into a 50 ml of either Cu (II) nitrate (0.1-0.9 ppm) or Ni (II) nitrate solutions (1-3 ppm) under a constantly stirring condition at room temperature. The pH value of the solutions was adjusted to 4.0 for each experiment. Subsequently, the aqueous phase was separated by filtration and the amount of the remaining Cu (II) and Ni (II) ions were determined by Flame Atomic Absorption spectroscopy (FAAS). The adsorbed amounts of metal ions were evaluated based on the difference of their initial and final concentrations. Powder X-ray diffractograms were recorded on a Bruker D8 Advance diffractometer, Cu $K_{\alpha 1}$ with PSD detector; 2θ range 5°-90°; step size 0.0154° and step time 1 second. FAAS measurements were performed on a Perkin-Elmer 3100 operating with Deuterium lamp background correction. Transmission electron micrographs were recorded on a TECNAI T20 electron microscope with the operating voltage of 80 KeV.

Results and Discussion

Fig. 1 demonstrates that the Ni catalyst used for synthesizing the MWNTs was effectively removed from their nanostructure as seen that none of the diffraction peaks corresponding to Ni appears in Fig. 1(b).

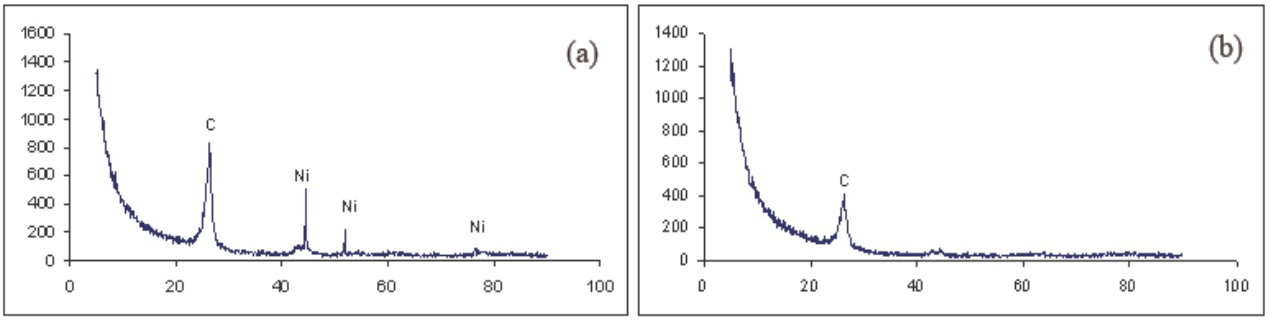

Fig.1. Powder XRD patterns of (a) as-received MWNTs and (b) cf-MWNTs

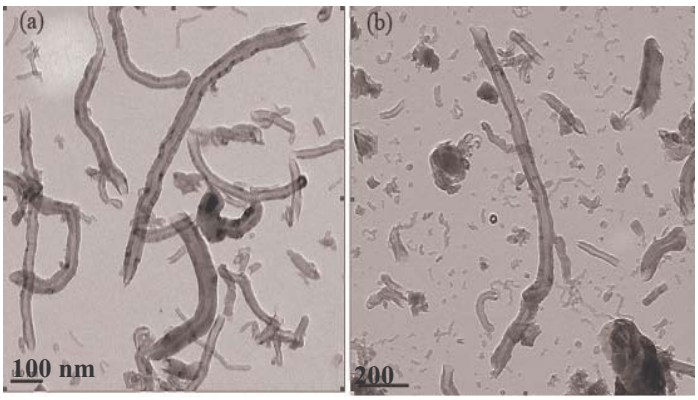

Fig. 2. TEM micrographs of (a) as received MWNTs and (b) mech-MWNTs

As shown in Fig. 2, the TEM micrograpgh of mech-MWNTs illustrated a relatively high fraction of shortened nanotubes in comparison to that of the as-received MWNTs. From greater than 50 TEM micrographs (each of which containing several nanotubes), the average outer- and inner- diameters and average length of the nanostructured materials were obtained and reported in Table 1.

The relatively small dimensions of mech-MWNTs indicated that the mechanochemical treatment dose not only shorten but also lessen the nanotubes. Nevertheless, TEM images showed that the mech-MWNTs is still of tabular structure with opened ends. According to an increase of the number open ends of the nanotubes, it should be able to assume that the surface area of mech-MWNTs is highest among three samples.

Table 1. Physical properties of the Carbon materials studied.

	Outer diameter (nm)	Inner diameter (nm)	Length (nm)
as-received MWNT	40	13	712
cf-MWNTs	43	16	859
Mech–MWNTs	32	13	208

Metal ions adsorption data were analyzed base on a several mathematical models, and it appeared that the isotherms data give an excellent fit with Langmuir theory,

$$S(ad) = N_{\max}\left(\frac{S(aq)}{K^{-1} + S(aq)}\right) \quad (1)$$

where *S(ad)* is number of ions adsorbed at the sites per unit area of the suface of MWNTs; *S(aq)* is the equilibrium concentration of ions in solution; $N_{\max}$ is the maximum adsorption capacity corresponding to a complete monolayer coverage on the surface of MWNT and K^{-1} is the Langmuir adsorption constant.

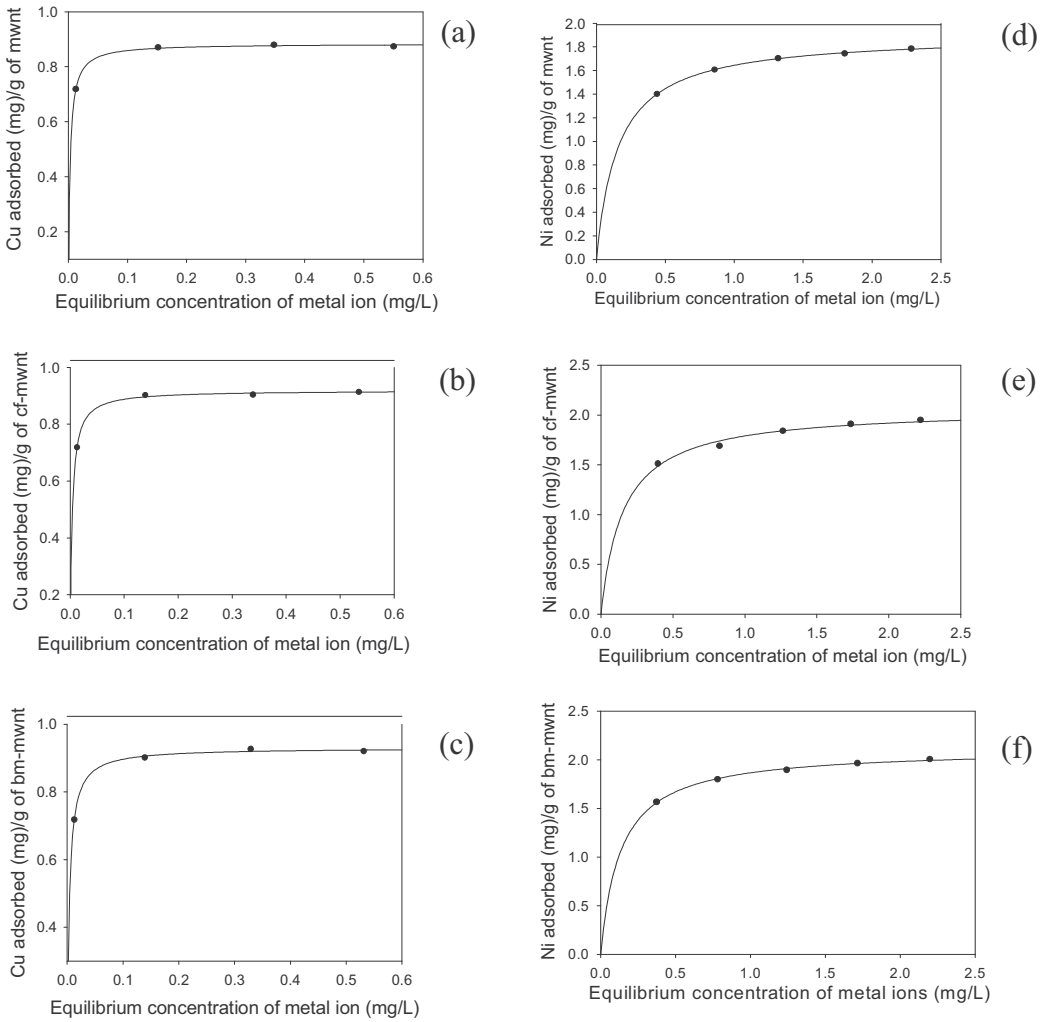

Fig. 3 Adsorption isotherm for Cu^{2+} on (a) MWNT (b) cf-MWNTs, (c) mech-MWNTs and the isotherms for Ni^{2+} on (d) MWNTs, (e) cf-MWNT and (f) mech-MWNTs.

The Langmiur data in Table 2 represent that the adsorption capacity of specific metal ions was not improved neither by the removal of catalyst nor by the mechanochemical treatment as seen in a slight

difference among the N_{max} of each MWNTs sample for each metal. However, the adsorption capacity of Ni^{2+} ions on the MWNTs material is twice higher than that of Cu^{2+} on the MWNTs.

Table 2. Comparison of Langmuir data for Cu^{2+} and Ni^{2+} ions on the MWNTs studied

Metal	Samples	N_{max} (mg/g)	K^{-1} (nmol/L)	R^2
Cu^{2+}	as-received MWNTs	0.88 ± 0.003	45 ± 2.0	0.9971
	cf-MWNTs	0.92 ± 0.004	55 ± 2.3	0.9974
	mech-MWNTs	0.93 ± 0.004	58 ± 2.5	0.9973
Ni^{2+}	as-received MWNTs	1.9 ± 0.01	2500 ± 51	0.9992
	cf-MWNTs	2.1 ± 0.03	2500 ± 310	0.9717
	mech-MWNTs	2.11 ± 0.01	2200 ± 850	0.9964

Summary

The mechanochemical treatment can shorten the MWNTs. The adsorption data of both Cu^{2+} and Ni^{2+} on all MWNTs materials were consistent with Langmiur behaviors. The MWNTs have appropriated sites for Ni^{2+} ions adsorbed on their outer surfaces of the tubes twice as much as they do for Cu^{2+}ions. The isothermal adsorption reported in this work implied that the mechanochemical treatment does not increase appropriate sites for the adsorption of metal ions.

Acknowledgment

This work was supported by the Center of Innovation in Chemistry: Postgraduate Education and Research Program in Chemistry (PERCH-CIC), Thailand Research Fund (Grant #MRG5080059) and the Commission of Higher Education.

References

[1] S. Iijima: Nature, Vol. 354 (1991), p. 56.
[2] R.H. Baughman, A.A. Zakhidov, W.A. de Heer: Science, Vol. 297 (2002), p. 787.
[3] S.J. Tans, A.R.M. Verschueren, C. Dekker: Nature, Vol. 393 (1998), p. 49.
[4] A.C. Dillon, K.M. Jones, T.A. Bekkedahl, C.H. Kiang, D.S. Bethune, M.J. Heben: Nature, Vol. 386 (1997), p. 377.
[5] J. Kong, N.R. Franklin, C. Zhou, M.G. Chapline, S. Peng, K. Cho, H. Dai: Science, Vol. 287 (2000), p. 622.
[6] M. Cinke, J. Li, C.W. Bauschlicher Jr., A. Ricca, M. Meyyappan: Chem. Phys. Lett., Vol. 376 (2003), p. 761.
[7] C. Lu, H. Chiu, C. Liu: Ind. Eng. Chem. Res., Vol. 45 (2006), p. 2850.
[8] H.J. Wang, A.L. Zhou, F. Peng, H. Yu, L.F. Chen: Mater. Sci. Eng., Vol. A466 (2007), p. 201.
[9] P.A. Gauden, A.P. Terzyk, G. Rychlicki, P. Kowalczyk, K. Lota, E. Raymundo-Pinero, E. Frackowiak, F. Beguin: Chem. Phys. Lett., Vol. 421 (2006), p. 409.
[10] C. Lu, Y.L. Chung, K.F. Chang: Water Res., Vol. 39 (2005), p. 1183.
[11] P.singjai, S. Changsarn, S.Thongtem: Mat. Sci. Eng. A-STRUCT., Vol. 443 (1-2) (2007), p. 42.

click for feedback
consult - comment - contact

Elsevier Editorial System(tm) for Materials Chemistry and Physics
Manuscript Draft

Manuscript Number: MATCHEMPHYS-D-08-03036

Title: Hydroxyapatite/Collagen Composite and Its Applications as Bone Filler and Drug Carrier

Article Type: Full Length Article

Keywords: Biomaterials; Chemical synthesis; Microstructure; Drug carrier

Corresponding Author: Dr. SIWAPORN MEEJOO, Ph.D

Corresponding Author's Institution: MAHIDOL UNIVERSITY

First Author: SIWAPORN MEEJOO, Ph.D

Order of Authors: SIWAPORN MEEJOO, Ph.D; WEERAPHAT PON-ON, Ph.D; TAWEECHAI AMORNSAKCHAI, Ph.D

Abstract: A one-step chemical reaction was carried out to obtain a hydroxyapatite/collagen (HAp/Col) composite. The porous HAp/Col material is of globular structure comprising HAp nanocrystals, which well stabilized on a rod-like, microcrystal platform. Formation of the composite was driven by the mineralization of HAp crystals and interfacial interactions between ions on the HAp surface and residual ions on the Col matrix. IR absorption bands corresponding to hydroxyl and phosphate groups provided convincing evidence of the mineralization of HAp in the Col matrix. In vitro bioactivity of the HAp/Col was examined by soaking the composite in a simulated body fluid (SBF) solution. Surface morphology of the HAp/Col showed substantially large cavities which are of high potential for drug delivery applications. In this work, Vancomycin (VCM), an antibiotic, was well-stabilized within the pores and on the surface of the hybrid composite. Drug release behaviors and the possible drug release mechanisms of VCM from the HAp/Col were discussed. This work has suggested that the release of VCM depends on the stability of porous structure of the

composite from the results of a rapid drug release within 5 hours and a very slow release over a period of time after 5 to 30 hours.

Suggested Reviewers: Mark Hoffman
University of New South Wales
Mark.Hoffman@unsw.edu.au
Prof. Hoffman has a number of publication in Ceramic composites.

Mike Swain
University of Sydney
mswain@usyd.edu.au
Prof. Swain is an expert in Ceramic feild.

S K Pratihar
Department of Ceramic and Engineering, Rourkela
skpratihar@nitrkl.ac.in
Prof. Pratihar published some work about hydroxyapatite composites.

Opposed Reviewers:

Dear Editor,

Please find the enclosed manuscripts entitled 'Hydroxyapatite/Collagen Composite and its Applications as Bone Filler and Drug Carrier' and kindly consider publishing our work in your high-standard journal.

On behalves of the authors, I would like to confirm that
1. The article is original.
2. The article has been written by the stated authors who are ALL aware of its content and approve its submission.
3. The article has not been published previously.
4. The article is not under consideration for publication elsewhere.
5. No conflict of interest exists, or if such conflict exists, the exact nature of the conflict must be declared.
6. If accepted, the article will not be published elsewhere in the same form, in any language, without the written consent of the publisher.

The list of potential reviewers is given as follows.

1. Prof. Mike Swain
   Biomaterials Unit, Faculty of Dentistry, University of Sydney, NSW Australia
   Phone: +61 2 9351 1814 Fax: +61 2 9351 1815
   Email: mswain@usyd .edu.au

2. Prof. Mark Hoffman
   School of Materials Science and Engineering
   University of New South wales, NSW 2052, Australia
   Phone +61 2 9385 4432 Fax: +61 2 9385 5956
   Email : Mark.Hoffman@unsw.edu.au

3. Prof. SK Pratihar
   Department of Ceramics and Engineering, Rourkela 769008, India
   Email: skpratihar@nitrkl.ac.in

The manuscript is in Word XP and is named "SMeejoo_HApCol".
Thank you and I am looking forward to hearing from you.

Yours Sincerely,
Siwaporn Meejoo

Department of Chemistry
Faculty of Science, Mahidol University
Rama VI Road, Bangkok 10400

Tel: +662-2015164, Fax: +662-354-7151, Email: scsmj@mahidol.ac.th

* Manuscript
Click here to view linked References

Hydroxyapatite/Collagen Composite and Its Applications as Bone Filler and Drug Carrier

Siwaporn Meejoo*, Weeraphat Pon-On and Taweechai Amornsakchai
Department of Chemistry, Faculty of Science, Mahidol University, Bangkok 10400, Thailand

Abstract

A one-step chemical reaction was carried out to obtain a hydroxyapatite/collagen (HAp/Col) composite. The porous HAp/Col material is of globular structure comprising HAp nanocrystals, which well stabilized on a rod-like, microcrystal platform. Formation of the composite was driven by the mineralization of HAp crystals and interfacial interactions between ions on the HAp surface and residual ions on the Col matrix. IR absorption bands corresponding to hydroxyl and phosphate groups provided convincing evidence of the mineralization of HAp in the Col matrix. *In vitro* bioactivity of the HAp/Col was examined by soaking the composite in a simulated body fluid (SBF) solution. Surface morphology of the HAp/Col showed substantially large cavities which are of high potential for drug delivery applications. In this work, Vancomycin (VCM), an antibiotic, was well-stabilized within the pores and on the surface of the hybrid composite. Drug release behaviors and the possible drug release mechanisms of VCM from the HAp/Col were discussed. This work has suggested that the release of VCM depends on the stability of porous structure of the composite from the results of a rapid drug release within 5 hours and a very slow release over a period of time after 5 to 30 hours.

Keywords: Biomaterials, Chemical synthesis, Microstructure, Drug carrier

Corresponding author: SM Email: scsmj@mahidol.ac.th Tel: +66-2-2015164, Fax: +66-2-3547151

Introduction

Fabrications of composite hybrid materials have received an extensive interest to produce artificial hard tissues such as cartilage and bone. The highly organized structure of bones is derived from the mineralization of both inorganic constituent, hydroxyapatite (HAp), and organic macromolecule, collagen (Col). The HAp/Col composite hybrid material can be employed as an implantable material for correcting bone or tooth damage caused by accidents or diseases [1-3]. As the chemical formula of HAp is ($Ca_{10}(PO_4)_6(OH)_2$) [1-5] similarly to the mineral present in bones and teeth, the material becomes biocompatible after implantation in human body. In addition, since calcium phosphate ceramics and their ions are naturally present in the body, indicating their biodegradability [1, 2]. For decades, there have been extensive efforts to use composite hybrid materials to duplicate bones and their enviable mechanical properties such as high strength and fracture toughness because these properties arise from the unique incorporation between organic and inorganic compositions of bones. Nevertheless, the biomaterials used in orthopedic treatments are different drastically from natural bones. For instance, the biomaterials for total joint replacement are inert metal alloys and ceramics [1, 2] as well as some polymeric materials [6-8]. Many attempts have been carried out to synthesize composite materials of calcium phosphate (CaP) by incorporating metal ions [2] and introducing organic molecules such as polymers to enhance the biocompatibility and bioactivity of composites [6, 7]. It has been well known that natural bones contain collagen (Col) fibrils (~30% by weight) and that the CaP and HAp crystals grow and incorporate between collagen molecules, for which the ceramic crystals are regularly aligned along the Col matrix [1, 10]. Preparations of bone-like hybrid composite biomaterials have been widely developed mainly to integrate all possible properties suitable for orthopedic surgical treatments [9-18]. In addition, unsuccessful bone implants were often due to infection, as the implant can provide a region inaccessible to the body's immune system. Bacterial bone infections can be a significant obstacle for successfully orthopedic surgery. To facilitate a recovery from bone implant, patients are commonly prescribed antibiotics to avoid infection due to bacteria in open fractures as well as anti-inflammatory medication. An advanced solution to this problem would be the incorporation of these medications directly into the

biomaterials [19-23]. This research describes a one-step preparation of HAp/Col composite which is chemically similar to bone and teeth. Since the collagen in bone has a ropelike arrangement, we employed the collagen matrix as a template for the mineralization of HAp crystals. The HAp/Col hybrid composite was formed via a self-organization mechanism that was induced by carefully controlling the charge states of the functional groups on collagen ($-COO^-$ and NH_3^+) and hydroxyapatite (Ca^{2+} and PO_4^{3-}). Thus, the HAp crystals align on the Col template through electrostatic interactions in the ionic system. An *in vitro* bioactivity test on the composite was carried out and changes in the microstructure of the composite were investigated. Furthermore, it was shown that this porous HAp/Col composite is appropriate for drug delivery applications [25-29]. This practical use was confirmed by examining the microstructure of the composite and Vancomycin hydrochloride (VCM) incorporated therein. For the current study, VCM was selected as it has been used clinically to treat osteomyelitis infections in patients allergic to penicillin or to treat methycillin-resistant forms of *Stayphylococcusaureus* infections [21, 27-28]. As a result, the antibiotic containing HAp/Col composite may suitably release the medicinal exipient in an open fracture, providing an aseptic surgical treatment.

Experimental Methods

To prepare the HAp/Col composite, $CaCl_2$ (Fluka) and K_2HPO_4 (Fisher Scientific, UK) were used as precursors of calcium and phosphate, respectively. Collagen from calf skin (Sigma, USA) acted as an organic template to form rod-like HAp structures and to inhibit excessively rapid growth of HAp crystals on the Col matrix. Throughout the reaction, pH was kept at ~9 by adding NH_4OH (J.T. Baker, USA). The formation of HAp on the Col matrix was initiated via a co-precipitation process from solution at room temperature. The HAp/Col growth occurred through self-organization between ions on Col, carboxyl group ($-COO^-$) and amino group (NH_3^+), and HAp, calcium (Ca^{2+}) and phosphate (PO_4^{3-}) ions. Note that de-ionized water has been used as solvent throughout this work. First, 10 ml of 0.24 M of K_2HPO_4 solution was added to a 3g/L of Col solution. Then, the mixture was continuously stirred for 20 minutes and kept at pH~9 throughout the reaction by adding extra NH_4OH. At this stage, electrostatic interactions between NH_3^+ from the Col matrix and PO_4^{3-} ions are predicted to occur. Next, 10 ml of

0.4 M $CaCl_2$ was gradually dropped into the previous mixture and white precipitate of the HAp/Col composite then formed. The precipitate was continually stirred for one hour, and was washed using de-ionized water until the supernatant reached pH~7. Then, the wet precipitate was transferred into a Petri dish and solvent was completely removed under freeze drying. Diffraction patterns for all samples were recorded on a Bruker powder diffractometer (Model D8 Advance) using Cu Kα1 radiation, operating at 40kV and 40 mA current, over a range $2\theta = 20^{o}$ to 60^{o} scan using a scanning speed of 1 second/step with an increment of 0.037^{o}. IR spectra were measured on an FT-IR spectrometer (Spectrum GX, Perkin Elmer (USA)) using the KBr pellet technique. A scanning electron microscope (JEOL model JSM-6301F) was used with an accelerating voltage of 15 kV to observe the microstructure of the composite samples before and after the bioactivity test and after drug-loading. To study the bioactivity of HAp/Col composite, the composite pellet (dimension of 10 mm in diameter and ~4 mm in thickness) was soaked in a simulated body fluid (SBF). This fluid has an ionic composition and pH similar to those of human plasma. In order to prepare a SBF solution, one needs to get the concentration of a number of electrolytes in an aqueous solution as follows; NaCl (136.8 mM), $NaHCO_3$ (4.2 mM), KCl (3.0 mM), K_2HPO_4 (1.0 mM), $MgCl_2{\cdot}6H_2O$ (1.5 mM), $CaCl_2$ (2.5 mM) and $NaSO_4$ (0.5 mM). *In vitro* tests were conducted by immersing the composite pellet in 50 ml of SBF for one week at 37 ºC under static condition. The SBF solution was replaced every three days to avoid any change in the cationic concentration that may occur due to degradation of the samples. After immersion in the SBF, the pellet sample was washed with de-ionized water before any further characterization.

Drug-loaded HAp/Col composite was prepared in order to study the drug-release behavior of the composite. Here, 100 mg of the HAp/Col powder was immersed in a 50mg/ml aqueous solution of Vancomycin (VCM) (Fluka, Biochemika). The mixture was incubated under stirring condition at 37 °C for 48 hours. Next, freeze-drying was performed to remove water resulting of the VCM loaded composite. An *in vitro* study of the release of antibiotic from the composite was monitored as follows. To study the behaviors of the stabilized VCM in the composite, the powder of the VCM loaded composite was dispersed in a 15 ml of phosphate buffer (Fisher Scientific, UK), and kept

at pH~7 and at 37 °C. Then, the suspension was placed in a shaking bath (SKAKER, Sk-300) operating with a rotating speed of 80 rpm for varied incubation times, 0.5, 2, 4, 6, 8, 10, 20 and 30 hours. After the incubation, the composite was separated from the mixture by centrifugation. To measure the released drug content, 3 ml of the supernatant was taken out to perform an absorption measurement at wavelength 280 nm for an assessment of the VCM concentration [31] on a UV-Vis spectrophotometer (Jenway, model 6405). Drug content was determined using a calibration curve of the VCM standard solution in Fig 6. In order to determine the remaining VCM content in HAp/Col, the separated samples were suspended in the phosphate buffer, for which the mixture was vigorously stirred for 1 hour, following by centrifugation. Subsequently, absorption property of the supernatant was measured.

Results and Discussion

Characterization of the HAp/Col composite

Figure 1(a) represents the powder X-ray diffraction pattern of hydroxyapatite prepared by using similar method used to prepare HAp/Col, except no adding collagen. The powder XRD in Fig. 1(a) is a typical pattern for a single phase hydroxyapatite (XRD JCPDS data file NO. 9-432). Powder XRD of the as-prepared HAp/Col composite and the SBF-treated HAp/Col are shown in Fig 1(b) and Fig 1(c) respectively. Figure 1(b) reveals that the powder XRD of HAp/Col composite is slightly different from that of hydroxyapatite. However, few strong diffracted peaks (2θ ~26° and 39°) and fairly weak peaks (over the 2θ range of 30-35°) clearly indicate a severe “preferred orientation” of the HAp crystals incorporated in the Col matrix. It should be pointed out that Col also gave a broad feature at 2θ ~10-20°, indicating an amorphous phase. Figure 1(c) implied a less severe preferred orientation in the SBF soaked HAp/Col sample. However, a broad XRD feature shows a possibility of mixed crystalline phases. Chemical functional groups of the HAp/Col composite and chemical interactions between the organic and inorganic components were confirmed by IR spectroscopy. IR spectrum of the HAp/Col in Fig. 2(a) represents strong absorption bands in the range of 3310-3450 cm^{-1} corresponding to overlapping signals generated by the O-H group of HAp and the N-H group of collagen. The characteristic bands at about 2900 cm^{-1} and 900 cm^{-1} respectively correspond to

stretching and bending vibration modes of the C-H groups of collagen. The broad absorption bands at 3416 cm^{-1} and 1637 cm^{-1} correspond to moisture on the composite surface. Moreover, intense bands at 1088 cm^{-1}, 1035 cm^{-1} and 961 cm^{-1} correspond to the $(PO_4)^{-3}$ stretching modes, while a doublet at 602 cm^{-1} and 562 cm^{-1} is due to the $(PO_4)^{-3}$ bending mode. Note that an absorption peak at 1383 cm^{-1} is an evidence of the $(NH_3)^{+}$ group in the Col matrix. In addition, the broadening of IR bands at 1088 cm^{-1}, 1035 cm^{-1} and 961 cm^{-1} correspond to the $(PO_4)^{-3}$ stretching modes of HAp and possibly indicate some distortion in the HAp structure. By carefully comparing the IR spectrum of HAp/Col composite and those of HAp reported earlier [24], one can conclude that the shoulder signals around 1450 cm^{-1} and 1640 cm^{-1} and the doublet peaks around 873 cm^{-1} are characteristic of carbonated ions substituted on the phosphate site in an apatitic structure, so called B type apatite. More importantly, the absorption peaks detected at around 1629 cm^{-1} and 1510 cm^{-1} typically represent amide I (C=O bond) and amide II (C─H bond) bands, respectively. It should be noted that the intensity of the amide I peak is higher than that of the amide II peak, which may indicate that negatively charged groups such as the carbonyl groups (COO^{-}) of the Col initiated the HAp nucleation and allowed the crystal growth on the Col matrix [17]. This phenomenon resembles the bionic growth of HAp crystals in natural bone during bio-mineralization.

The morphology of HAp/Col composite at the top surface and the platform are shown as SEM and TEM results in Fig 3. Figure 3(a-b) represent SEM micrographs of the top surface of the HAp/Col composite, where as Fig. 3(c) represents the microstructure at the platform of the composite. The top surface of the composite shows a globular shape with big cavities in which the HAp crystals have embedded in the Col matrix. There are also pores between each globular particle. High-resolution SEM images of the composite (Fig. 3 (b)) clearly showed a relatively large empty space at the surface of composite. Figure 3(b) shows the pedestal parts of the composite representing rod-like HAp crystals with dimensions of about 1 μm in width and 6-8 μm in length. Note that the orientations of these crystals are almost in the same direction and it is consistent with X-ray diffraction result which confirms “preferred orientations” of the HAp crystals on the Col matrix. The formation of rod-like structures may be due to crystal growth of the HAp phase on the Col matrix by self-organization process. This self-organization could be

attributed to electrostatic interactions between ions of opposite charge contributed by Col ($-COO^-$ and NH_3^+) and HAp (Ca^{2+} and PO_4^{3-}). IR measurements on pure Col, pure HAp and the composite have confirmed the above described interactions.

In addition, the peak broadening of XRD result can be used to estimate the crystalline size in a direction perpendicular to the crystallographic plane based on Scherrer's formula, $d = k\lambda/\beta\cos\theta$ [18]. Where d is the average crystalline size, λ represents the wavelength of X-ray radiation (0.154056 nm), k is a constant related to the crystallite shape and is approximately equal to unity. β is the full width of the peak at haft of the maximum intensity (rad) and θ is the Bragg' angle. As a result, from the (002) diffraction peak ($2\theta = 26^o$) using Scherrer's equation, the average size of HAp crystallite of the HAp/Col composite 6.36 nm, consistent with the TEM result (Fig 3(d)) which shown the plate-like nanostructure of HAp/Col composite.

In vitro bioactivity test

After soaking the HAp/Col pellet in SBF for 7 days, a deposition of calcium phosphate of apatite crystals was detected, as shown in the cleared diffraction pattern (Fig. 1(b)) and in SEM micrographs (Fig. 4). Although all diffracted peaks are corresponding to a single crystalline phase of HAp, the peaks are fairly broad and not well-resolved compared to those seen in the literature [1, 2]. The broad diffraction peaks in Fig. 1(c) may indicate that either the deposited phase does not perfectly crystallize or that the crystals are very small. As shown in Fig. 4, after immersion in SBF, there has been an agglomeration of tiny crystals on the surface of the composite. Besides, a number of diffraction peaks from the SBF immersed composite indicated less preferred orientation of HAp crystals formed on the HAp/Col surface.

The relatively high content of HAp crystal on the immersed composite is confirmed by dominant IR bands corresponding to HAp phase, shown in Fig 2(b). The IR spectrum was composed of absorption bands typically associated with B type apatite. It should be pointed out that the asymmetric stretching vibration of a dissociated carboxyl group ($-COO^-$) observed at 1629 cm^{-1} for HAp/Col (Fig. 2(a)) shifted to a higher wavenumber (1642 cm^{-1}) after soaking in SBF (Fig. 2(b)). This result implied that the bond in that particular $-COO^-$ group was weakened because of the formation of a new

chemical bond between Ca^{2+} ions on the HAp surface and COO^{-} on Col [17, 18]. For this reason, it can be concluded that the nucleation of HAp crystals on a Col matrix is critically dependent on the charged functional groups at the Col surface.

The micrographs in Fig. 4 revealed that the surface of the HAp/Col composite, after immersion in SBF, comprised of a honeycomb-like structure with irregular pores and irregularly shape of agglomerated particles about 2-5 μm in diameter on the specimen. This result indicate the formation of *in vitro* nucleation of HAp crystals, and hence bioactivity of the HAp/Col composite. SEM/EDS spectroscopy has been carried out to identify chemical compositions of the HAp/Col and the particle deposited on the composite after immersion in SBF. EDS studies reveal deposition of ion deposition on the composite surface after in *vitro* bioactivity test. Table 1 reported that the concentration ratios of Ca/P of the HAp/Col composite and the deposited particle are equal to 1.71 and 1.62 respectively. Note that these values are quite close to the Ca/P ratio of HAp and non-stoichometric HAp [1]. As the result, it can be concluded that new HAp crystals are formed after immersion of the HAp/Col composite in SBF. Similar phenomena are expected under *in vivo* conditions, i.e. new HAp like phase should form on the surface of the HAp/Col composite after its implantation into human body.

In vitro release

VCM loaded HAp/Col particles were obtained by impregnation method. The incorporation of VCM within the HAp/Col structure was monitored from SEM micrographs as shown in Fig. 5. It is clear that the globular structure remains, after drug loading, but that the porosity of the structure (Fig. 5 (b)) has decreased. A gel-like film of VCM was observed on the composite surface, probably due to the presence of excess VCM. Higher magnification micrographs (Fig. 5 (b-c)) revealed that the surface of the HAp/Col is completely covered with a VCM layer. This is a strong indication that VCM is well-incorporated within pores of the composite. In addition, the deep pockets between each globular particle that were seen in Fig 3(a) have become groove-like features after drug loading (Fig 5 (b)). Instead of a porous surface structure, the surface appears to be much smoother in Fig 5 (c). The view in Fig. 5 (c) may represent an area on the HAp/Col

that has been heavily loaded with VCM, which, in turn, might suggest that this composite has a high capacity for drug delivery applications.

For the drug release study from the composite materials, the concentrations of VCM released from the HAp/Col composite was determined using a calibration curve of VCM of standard concentrations, for which, the relationship between absorbance and the concentration of VCM can be describe in equation (1)

$$C_i = 0.1042A_i + 0.00018; R^2 = 0.9907 \quad (1)$$

;where C_i is the VCM concentration and A_i is the UV-Vis absorbance at a wave length of 280 nm. The release profile of VCM incorporated in HAp/Col composite is shown in Fig 6. One can observe a fairly rapid release of VCM during the first five hours and that the cumulative percent release of VCM from the HAp/Col composite reached around 48.7%, probably because the immediate dissolution of the excess VCM at the composite surface. After that, much slower release is noticed as seen by a slight increase (3-4%) of the cumulative percent release resulting of the net percentage was not greater than 50% over a period of 30 hours studied. More importantly, a gentle slope at 30 hours suggests that the release is going to carry on slowly. The porous structure of HAp/Col composite should play a very important role to the release behavior of any drug therein, as VCM can be incorporate within the collagen matrix by filling pores of the polymer through capillary forces and that might slow down the diffusion rate of VCM from the composite into the release medium (in this case, phosphate buffer). Nevertheless, the mechanism of drug release from a composite material can be very complex and involve a number of factors including porosity and pore structure of the matrix, relaxation, and release behaviors through the matrix.

Drug release kinetics can be examined in order to identify the release mechanism of VCM from the composite HAp/Col. By using Peppas model [30]:

$$\frac{M_t}{M_0} = kt^n \quad (2)$$

or

$$\ln\left(\frac{M_t}{M_0}\right) = n\ln t + \ln k \quad (3)$$

where M_0 and M_t are respectively initial concentration of drug in carriers and the time dependent concentration of drug released in medium at time t. Thus, M_t/M_0 is the fractional of drug release while k is a rate constant, which depends on the structural and geometric characteristic of the samples such as the surface area of the particles, diffusivity of the drug solubility, concentration of drug and porosity [22, 29]. The calculated exponent n is a characteristic index related to mode of drug transport. If n = 0.5 the kinetic behavior of drug release is described by Higuchi model [31] when a drug releases from a homogeneous matrix-type delivery system. The process is diffusion-controlled and is evidenced by proportionality between the amount of drug being released and the square root of time. From (3), the empirical components, n and k, of VCM being released from the HAp/Col composite can be obtained from the best fitting curve provided by the Peppas model and from the slope of ln (M_t/M_0) plotted against ln t in Fig 6(b). It is clear from Fig. 6 that the change in gradient of ln (M_t/M_0) occurs around t = 5 hours of release. For t between 0.5 to 5 hours, the exponent and rate constant can be estimated, n_1 = 0.65 for k_1 = 15.52, which indicate an intermediate mechanism between a diffusion-controlled process and a swelling-controlled process [30]. Swelling-controlled release generally occurs when diffusion of drug is faster than hydrogel swelling. Thus, the deformation of HAp/Col structure, or more specifically the changes of Col's pore size, played an important role to the kinetics of drug release. On the other hand, over the period of t >5 to t =30 hours, the calculated exponent n_2 = 0.05 for k_2 = 44.88, and that the very low n value reflects the very slow diffusion of VCM from the composite [30]. From this experiment, the release of VCM from the HAp/Col composite deviated from the Higuchi model [31] ($M_t = M_0 k t^n$, n = 0.5) where the results are discussed as follows. Within five hours, the release rate depends on the excess VCM loaded on the composite surface, including the deformed pore structure of the composite as the diffusion of drug occurred through the composite's pores. Instead, over the period of time after 5 hours to 30 hours studied, the relatively low release rate may results from some changes of the pore structure of collagen matrix upon swelling process, i.e pores closed and VCM was trapped therein.

Conclusion

The HAp/Col composite was prepared by a direct co-precipitation technique via the self-organization mechanism between HAp and collagen matrix. The composite demonstrated excellent biocompatibility after soaking in SBF. Due to the globular shaped microstructure including its high porosity, the HAp/Col material prepared here holds promise as a candidate for drug delivery. Analysis of drug release behavior from the composite confirms a significant potential to use the HAp/Col composite in biomedical applications, i.e bone replacement and aseptic surgical treatment.

Acknowledgements

This work was financially supported by the Commission of Higher Education and Thailand Research Fund (Grant #MRG5080059). Authors are also grateful for the support of the Center of Excellence for Innovation in Chemistry, Mahidol universiy. SEM measurements were made with the assistance of Jirawadee Thanatnit, Center of Nano-imaging (CNI) and Sumalee Charnchai, Faculty of Science, Mahidol University.

References

[1] S.V. Dorozhkin and M. Epple, Angew. Chem. Int. Ed. 41(17) (2002) 3130.

[2] P.N. Kumta, C. Sfeir, D.H. Lee, D. Olton and D. Choi, Acta Biomater. 1 (2005) 65.

[3] M. Sato and T.J. Webster, Expert. Rev. Med. Devic. 1(1) (2004) 105.

[4] H. Liu and T.J. Webster, Biomaterials. 28 (2007) 354.

[5] X. Wang, J. Zhuang, Q. Peng and Y. Li, Adv. Mater. 18 (2006) 2031.

[6] Y. Kong, W. Jie, W.C. Yuan and L. YuBao, Chinese Sci. Bull. 52(2) (2007) 267.

[7] P. Monvisade, P. Siriphannon, R. Jermsungnern and S. Rattanabodee, J. Mater. Sci: Mater. Med. 18 (2007) 1955.

[8] J. Venugopal, P. Vadgama, T.S. Sampath Kumar and S. Ramakrishra, Nanotechnology. 18 (2007) 055101.

[9] D. Wahl and J.T. Czernuszka, Eur. Cell. Mat. 11 (2006) 43.

[10] S. Liao, M. Ngiam, F. Watari, S. Ramakrishna and C.K. Chan, Bioinsp. Biomin. 2 (2007) 37.

[11] S. Kamakura, K. Sasaki, T. Homma, Y. Honda, T. Anada, S. Echigo and O.

Suzuki, J. Biomed. Mater. Res. 83A (2007) 725.
[12] D.A. Wahl, E. Sachlos, C. Liu and J.T. Czernuszka, J. Mater Sci: Mater. Med. 18 (2007) 201.
[13] J.H. Song, H.E. Kim and H.W. Kim, J. Biomed. Mater. Res. Part B: Appl. Biomater. 83B (2007) 248.
[14] D. Lickorish, J.A.M. Ramshaw, J.A. Werkmeister, V. Glattauer and C.R. Howlett, J. Biomed. Mater. Res: 68A (2004) 19.
[15] S. Sotome, T. Uemura, M. Kikuchi, J. Chen, S. Itoh, J. Tanaka, T. Tateishi and K. Shinomiya, Mat. Sci. Eng. C.-Bio. S. 24 (2004) 341.
[16] M. Kikuchi, H.N. Matsumoto, T. Yamada, Y. Koyama, K. Takakuda and J. Tanaka, Biomaterials. 25 (2004) 63.
[17] M. Kikuchi, S. Itoh, S. Ichinose, K. Shinomiya and J. Tanaka, Biomaterials. 22 (2001) 1705.
[18] R. Murugan and S. Ramkrishna, Appl. Phys. Lett. 88 (2006) 193124.
[19] J. Schnieders, U. Gbureck, R. Thull, T. Kissel, Biomaterials. 27 (2006) 4239.
[20] A.M. Le Ray, H. Gautier, M.K. Laty, G. Daculsi, C. Merle, C. Jacqueline, A. Hamel and J. Caillon, Antimcrob. Agents. Ch. 49(7) (2005) 3025.
[21] U. Gbureck, E. Vorndran, F.A. Müller and J.E. Barralet, J. Control. Release. 122 (2007) 173.
[22] V.C. Amaro Martins, G. Goissis, A.C. Ribeiro, E.M. Jr and M.R. Bet, Artif. Organs. 22(3) (1998) 2151.
[23] R. Murugan and K.P. Rao, Trends. Biometer. Artif. Organs. 16(1) (2002) 43.
[24] S. Meejoo, W. Maneeprakorn and P. Winotai, Thermochim. Acta 447 (2006) 115.
[25] B. Palazzo, M.C. Sidoti, N. Roveri, A. Tampieri, M. Sandri, L. Bertolazzi, F. Galbusera, G. Dubini, P. Vena and R. Contro, Mat. Eng. Sci. C-Bios. 25 (2005) 207.
[26] M. Sunder, N.R. Babu, S.P. Victor, K.R. Kumar and T.S. Sampath Kumar, Trends. Biometer. Artif. Organs. 18(2) (2005) 213.
[27] M.P. Ginebra, T. Traykova and J.A. Planell, J. Control. Release. 113 (2006) 102.
[28] A. Dion, M. Langman, G. Hall and M. Filiaggi, Biomaterials. 26 (2005) 7276.
[29] T.Y. Liu, S.Y. Chen, J.H. Li and D.M. Liu, J. Control. Release. 112 (2006) 88.
[30] N.A. Peppas and P. Colombo, J. Control. Release. 45 (1997) 35.

[31] T. Higuchi, J. Pharm. Sci**.** 52 (1963) 1145.

Figure Captions

Figure 1. XRD patterns of (a) HAp only, (b) HAp/Col composite and (c) HAp/Col composite after soaking in SBF solution for one week.

Figure 2. IR spectra of the HAp/Col composite; (a) HAp/Col and (b) HAp/Col after soaking in SBF fluid.

Figure 3. (a) SEM image at the top surface of HAp/Col, (b) at high magnification, (c) the microcrystal platform of HAp/Col composite and (d) TEM of nanocrystalline hydroxyapatite formed at the top surface of HAp/Col.

Figure 4. SEM image of the HAp/Col composite after soaking in a simulated body fluid (SBF) at 37°C for one week; (a), EDS profile of HAp/Col composite after soaking in one week SBF solution at two different site at (b) HAp/Col surface and (c) new HAp structure formed on HAp/Col surface.

Figure 5. Representative SEM images of the HAp/Col after a 48 h incubation with VCM. (a) SEM image at X3.0K. (b) and (c) SEM images at X10.0K at different positions.

Figure 6. VCM release process from the HAp/Col composite materials in solution of phosphate buffer pH=7. (a) ■ = data from experiment, — Fitting of the early release (below five hours) data to Eqn. (2) of text and – – – Fitting of Eqn. (2) to the latter time release (above ten hours) data.

Table 1. EDS result of the elements analysis of HAp/Col composite after soaked in 7 days SBF solution

Material	Weight concentration (%)							Ca/P
	C	O	Mg	P	Cl	K	Ca	Weight ratio
HAp/Col surface	**18.36**	**36.08**	**0.2**	**14.75**	**1.59**	**0.49**	**25.2**	**1.71**
Particles at surface	**27.71**	**35.38**	**0.28**	**11.47**	**1.12**	**0.47**	**18.53**	**1.62**

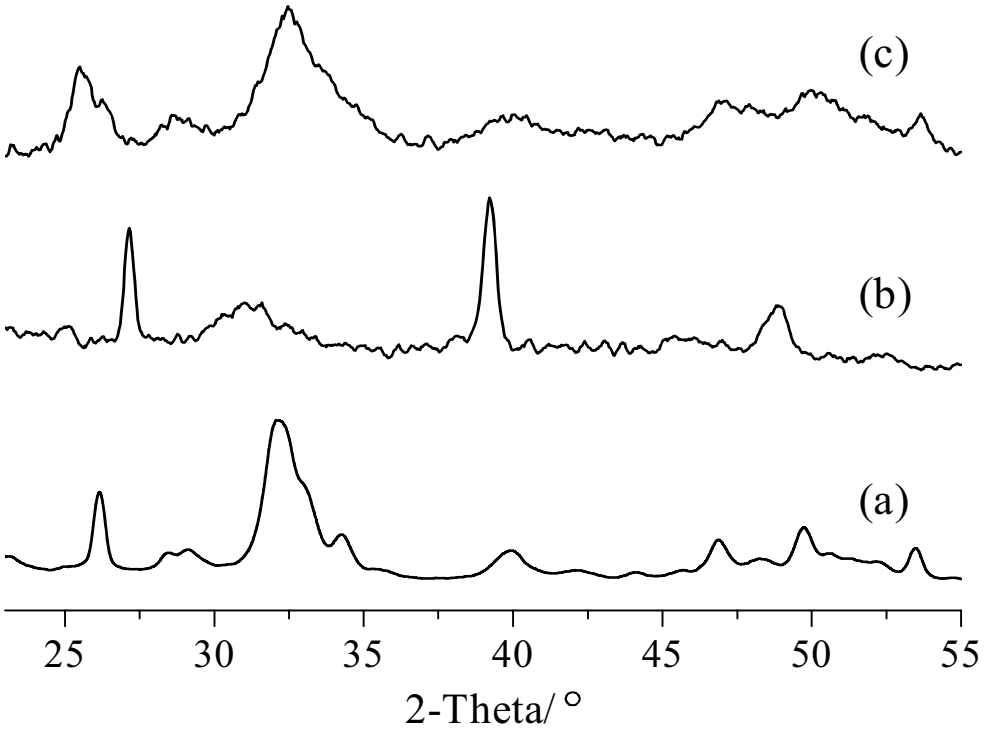

Figure 1.

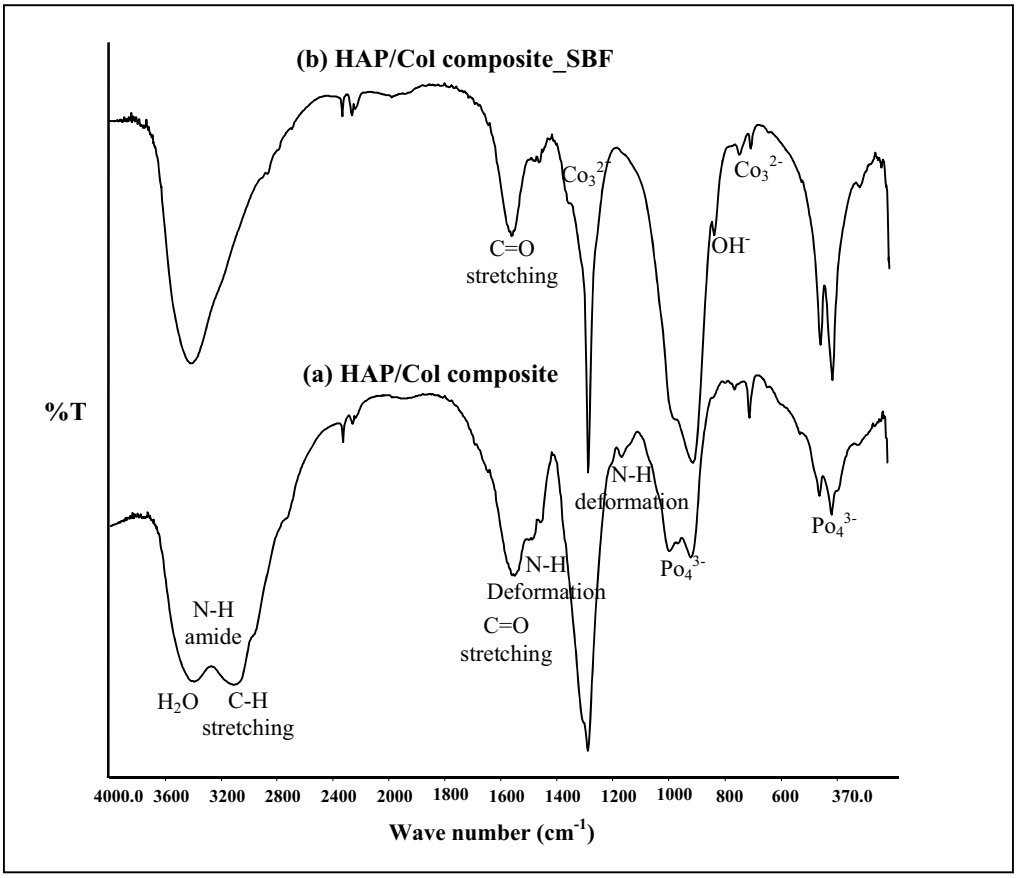
(b) HAP/Col composite_SBF
Co_3^{2-}
Co_3^{2-}
C=O
stretching
OH^-
(a) HAP/Col composite
%T
N-H
deformation
Po_4^{3-}
N-H
Deformation
Po_4^{3-}
N-H
amide
C=O
stretching
H_2O
C-H
stretching
4000.0 3600 3200 2800 2400 2000 1800 1600 1400 1200 1000 800 600 370.0
Wave number (cm^{-1})

Figure 2.

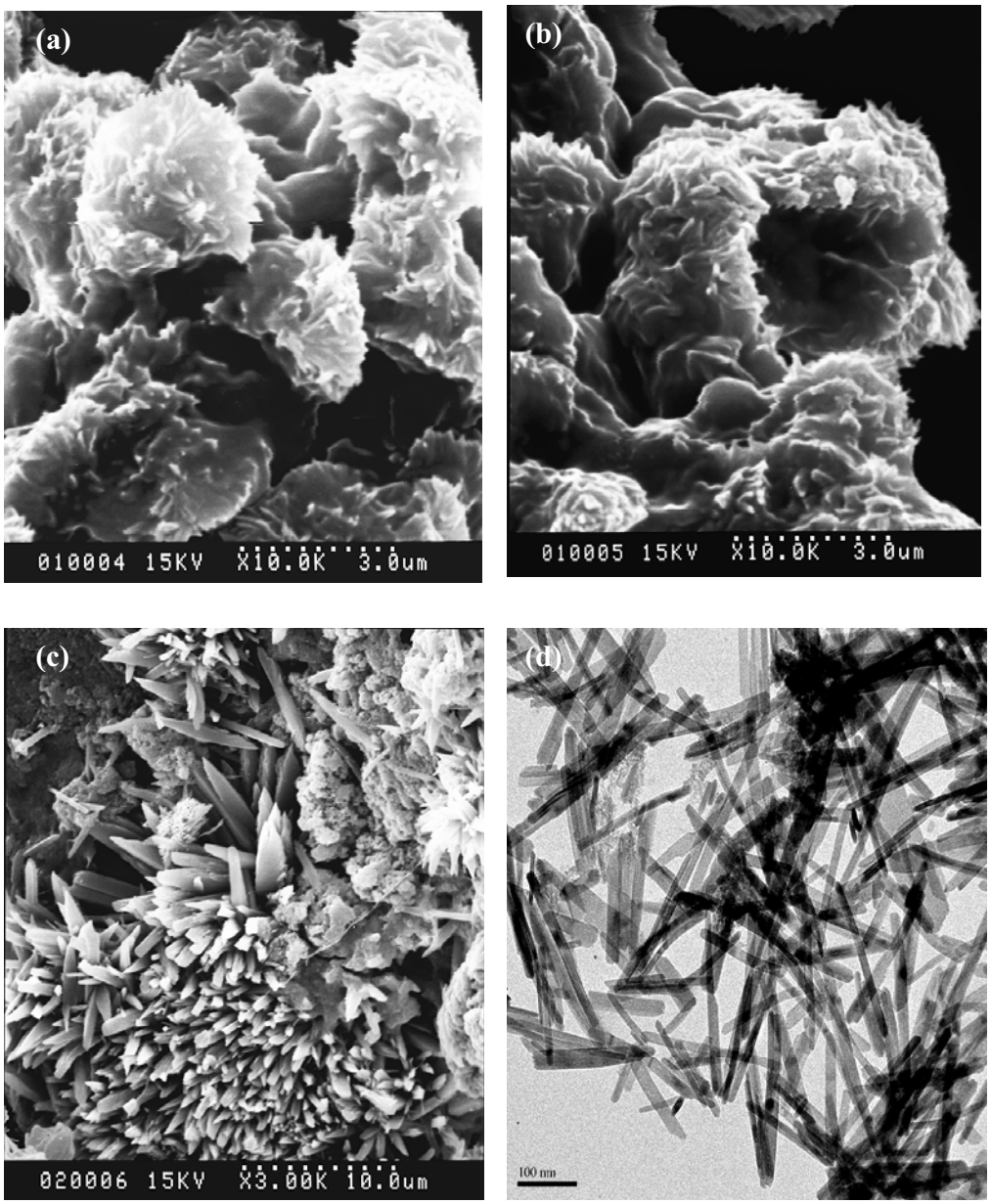
(a)
010004 15KV X10.0K 3.0um
(b)
010005 15KV X10.0K 3.0um
(c)
020006 15KV X3.00K 10.0um
(d)
100 nm

Figure 3.

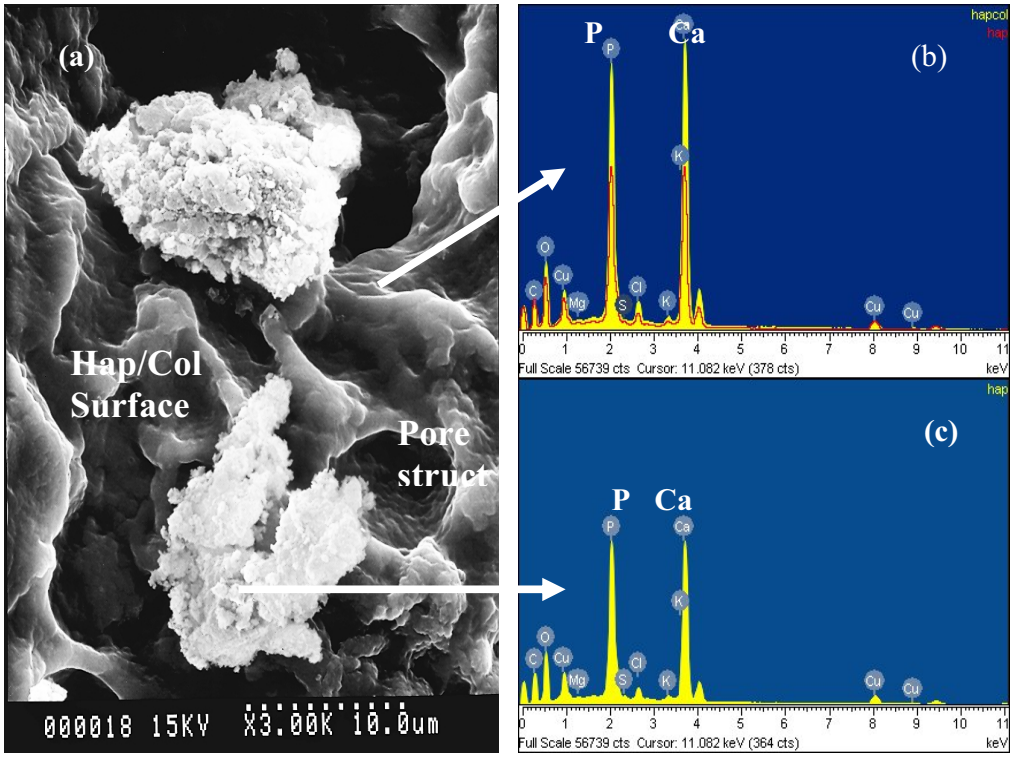
(a)
Hap/Col
Surface
Pore
struct
000018 15KV X3.00K 10.0um
(b)
P
Ca
hapcol
hap
Full Scale 56739 cts Cursor: 11.082 keV (378 cts)
keV
(c)
P
Ca
hap
Full Scale 56739 cts Cursor: 11.082 keV (364 cts)
keV

Figure 4.

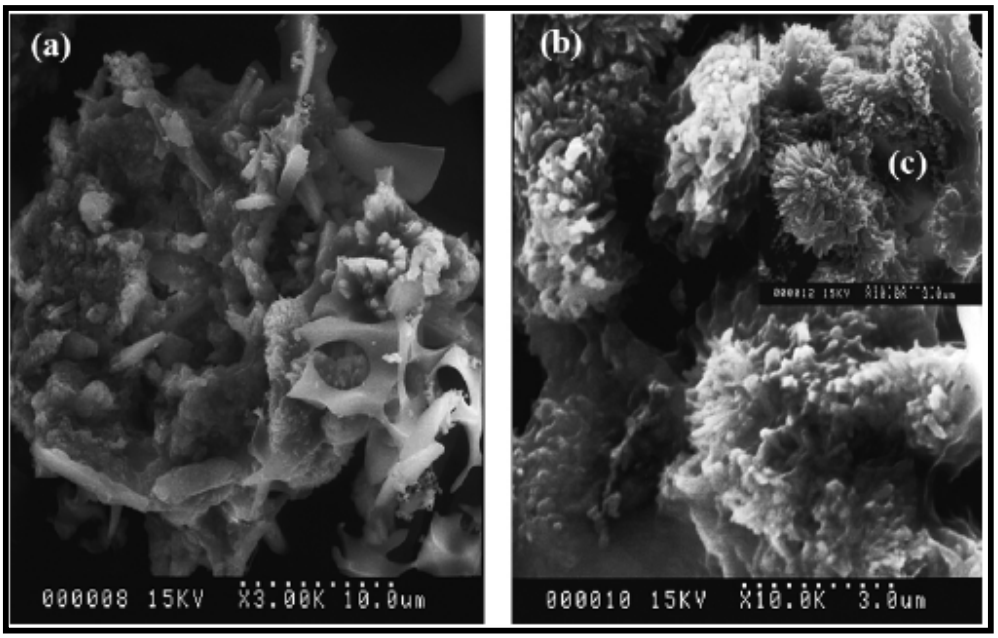

Figure 5.

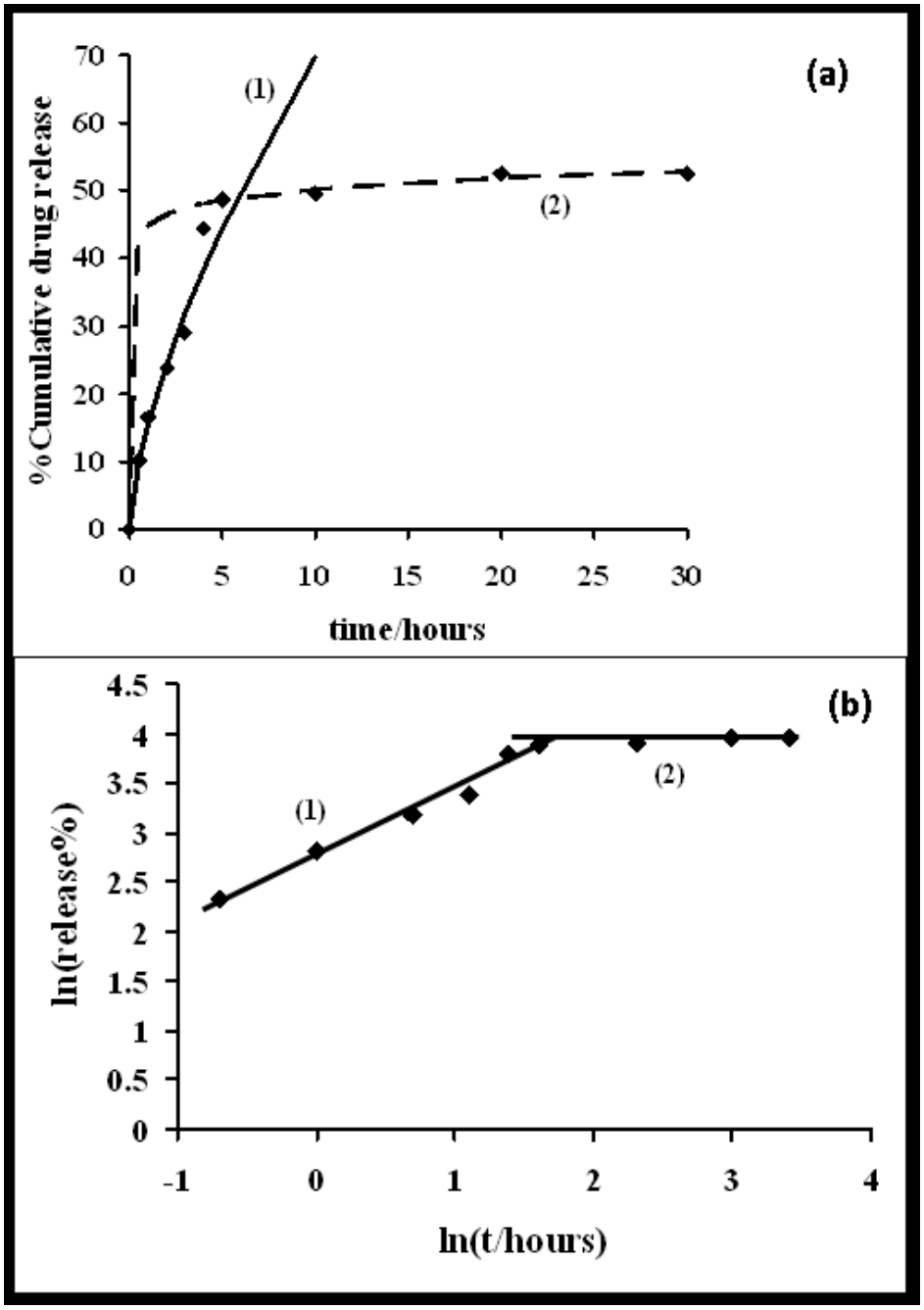
(a)
% Cumulative drug release
time/hours
(1)
(2)
0
10
20
30
40
50
60
70
0
5
10
15
20
25
30
(b)
ln(release%)
ln(t/hours)
(1)
(2)
0
0.5
1
1.5
2
2.5
3
3.5
4
4.5
-1
0
1
2
3
4

Figure 6.